Cell

Ricca's factors as mobile proteinaceous effectors of electrical signaling

Graphical abstract

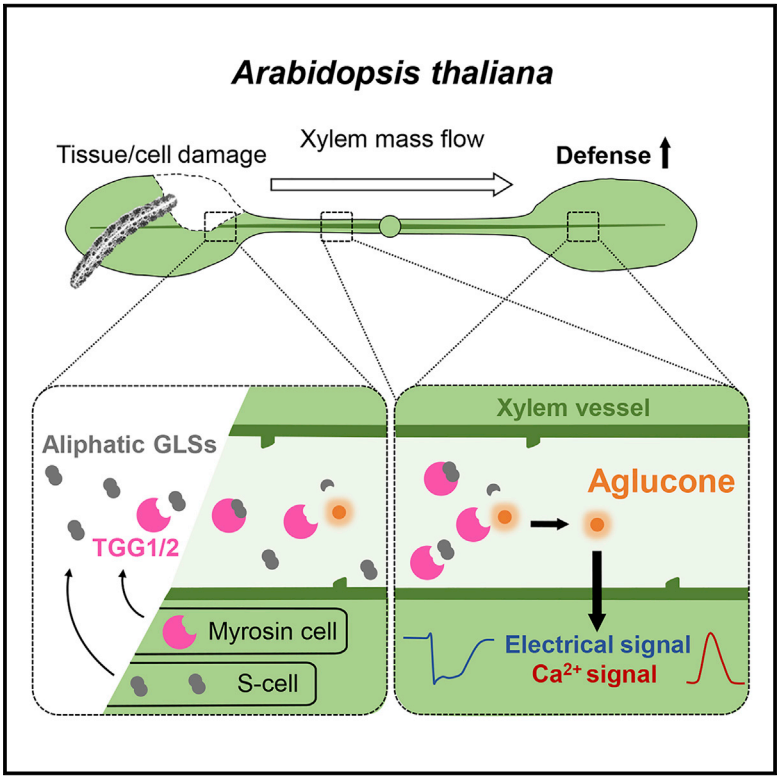

Authors

Yong-Qiang Gao, Pedro Jimenez-Sandoval, Satyam Tiwari, ..., Gaëtan Glauser, Julia Santiago, Edward E. Farmer

Correspondence

edward.farmer@unil.ch

In brief

β-THIOGLUCOSIDE GLUCOHYDROLASE 1 and 2 as xylem-mobile factors to generate membrane depolarizing elicitors in the veins of wounded *Arabidopsis*, highlighting a mechanism for inter-organ electrical signaling in wounded plants.

Highlights

- Leaf wounding triggers electrical signals that reach distal undamaged leaves
- Leaf-to-leaf electrical signal propagation depends on mobile glucohydrolase enzymes
- Glucohydrolase enzymes generate short-lived aglucone elicitors of membrane depolarization
- Inter-organ protein mobility underlies electrical signaling in a wounded plant

Gao et al., 2023, Cell *186*, 1337–1351
March 30, 2023
https://doi.org/10.1016/j.cell.2023.02.006

CellPress

Cell

CellPress
OPEN ACCESS

Article

Ricca's factors as mobile proteinaceous effectors of electrical signaling

Yong-Qiang Gao,[1] Pedro Jimenez-Sandoval,[1] Satyam Tiwari,[1,3] Stéphanie Stolz,[1] Jing Wang,[1] Gaëtan Glauser,[2] Julia Santiago,[1] and Edward E. Farmer[1,4,*]

[1]Department of Plant Molecular Biology, University of Lausanne, 1015 Lausanne, Switzerland
[2]Neuchâtel Platform of Analytical Chemistry, University of Neuchâtel, 2000 Neuchâtel, Switzerland
[3]Present address: Institute of Physics, School of Basic Sciences, École Polytechnique Fédérale de Lausanne, EPFL, 1015 Lausanne, Switzerland
[4]Lead contact
*Correspondence: edward.farmer@unil.ch
https://doi.org/10.1016/j.cell.2023.02.006

SUMMARY

Leaf-feeding insects trigger high-amplitude, defense-inducing electrical signals called slow wave potentials (SWPs). These signals are thought to be triggered by the long-distance transport of low molecular mass elicitors termed Ricca's factors. We sought mediators of leaf-to-leaf electrical signaling in *Arabidopsis thaliana* and identified them as β-THIOGLUCOSIDE GLUCOHYDROLASE 1 and 2 (TGG1 and TGG2). SWP propagation from insect feeding sites was strongly attenuated in *tgg1 tgg2* mutants and wound-response cytosolic Ca^{2+} increases were reduced in these plants. Recombinant TGG1 fed into the xylem elicited wild-type-like membrane depolarization and Ca^{2+} transients. Moreover, TGGs catalyze the deglucosidation of glucosinolates. Metabolite profiling revealed rapid wound-induced breakdown of aliphatic glucosinolates in primary veins. Using *in vivo* chemical trapping, we found evidence for roles of short-lived aglycone intermediates generated by glucosinolate hydrolysis in SWP membrane depolarization. Our findings reveal a mechanism whereby organ-to-organ protein transport plays a major role in electrical signaling.

INTRODUCTION

Deeply embedded in the vasculature, xylem vessels form low-pressure, fluid-filled continua spanning the bodies of plants.[1] When leaf veins are severed by feeding herbivores, fluid tension in the xylem is released suddenly.[2] Damaged vessels can, in theory, aspirate chemical mediators released from wounds, or from the herbivores themselves, and transport these compounds over long distances. Support for this comes from the observation of notodontid caterpillars that sever leaf stems (petioles) and then paint the cut ends with red saliva. The red salivary components are sucked into the xylem in a mechanism that may suppress long-distance defense signaling in the host trees.[3] More generally, components derived from the wounded plant are likely to enter the xylem. Indeed, the idea that xylem vessels could traffic defense mediators of plant origin dates back over a century to a classic paper by Ricca.[4] In that work, Ricca stated that xylem-borne "hormones" were transported from wounds to trigger distal leaf movements in the sensitive plant *Mimosa spegazzinii* (now *Mimosa polycarpa* var. *spegazzinii*). Later work extended the "Ricca factor" hypothesis to explain the spread of long-duration wound-response membrane depolarizations in other plants.[5] However, the nature of chemical mediators of inter-organ electrical signaling in plants remains unknown. By contrast, several key ion channels are known to control long-distance electrical signaling in leaves. Among these are several clade 3 GLUTAMATE RECEPTOR-LIKE (GLR) channels,[6] two potassium-selective channels (AKT2 and GORK),[7] and the mechanosensitive channel MSL10.[8] At the cell level, GLR populations were found in both the xylem and phloem. Both of these vascular tissues are critical for leaf-to-leaf electrical signaling in wounded plants.[9] Being potential gating ligands for clade 3 GLRs, amino acids such as glutamate are candidate elicitors of wound-response signaling. Exogenous glutamate triggers large cytosolic Ca^{2+} transients,[10,11] and this amino acid also excites the generation of slow wave potential (SWP)-like electrical signals.[12] However, genetic approaches have not yet demonstrated roles of amino acids as mediators of leaf-to-leaf electrical signaling. In the present work, we sought chemical mediators involved in leaf-to-leaf SWP signaling when *A. thaliana* was attacked by live herbivores.

SWPs are widespread if not universal electrical signals in angiosperms.[13] Triggered by severe wounding, these signals can be monitored with non-invasive surface electrodes. In *Arabidopsis*, SWPs move through primary veins in leaves distal to wounds at apparent velocities of approximately 8 cm per min.[6,14] This velocity is controlled, at least in part, by the xylem. Specifically, xylem cell wall integrity mutants both slow SWP velocities and

change their architectures. This was interpreted as being consistent with the transport of membrane depolarization elicitors through vessels.[14] The defining feature of the SWP is a long-duration (typically approximately 2 min) membrane depolarization phase that follows rapid, spike-like loss of membrane potential. Ricca's factors have been implicated specifically in the long-duration membrane depolarization phase of the SWP.[5] This is of interest because the duration of membrane depolarization determines the strength of the plant defense response.[15] In a search for Ricca's factors, we targeted this phase of the SWP. For this, we performed experiments in which leaf 8 of adult-phase plants was wounded by caged herbivores in order to trigger SWPs that spread to distal leaf 13.

RESULTS

Ricca's factors mediate wound-response SWPs in *Arabidopsis*

SWP electrical signals (Figure 1A) that are transmitted from leaf to leaf are induced when herbivores bite through a leaf midrib or petiole.[14] To define which tissues needed to be severed in order to generate the long-duration membrane depolarization phase that typifies the SWP, the petiole of leaf 8 was cut sequentially at 100-μm intervals (Figure 1B). During this procedure, electrical activity was monitored with non-invasive electrodes placed on the basipetal petiole of the cut leaf and on the petiole of distal leaf 13. Cutting either side of the primary vein often resulted in short-duration action potential-like depolarizations in the damaged leaf (Figure 1C). However, the long-duration membrane depolarizations that are typical of the SWP were only elicited in the distal leaf when the primary vein was severed (Figure 1C). This finding was of interest since elicitors of wound-response membrane depolarization in *Arabidopsis* were proposed to be drawn along veins from leaf to leaf via xylem vessels.[16]

To investigate leaf-to-leaf mass transfer and assess the velocity of wound-response mass transfer between leaves, the petiole of leaf 8 was cut in a solution of fluorescein (Figure 1D). Within 60 s, fluorescein was observed in connected leaves (Figure 1E), and the velocity of fluorescence transport into the distal leaf was similar to that of wound-response SWP propagation (Figures 1F and 1G). Clade 3 GLR proteins in plants control SWP signaling.[6] Using *glr* mutants, we investigated whether fluorescein transport could occur independently of GLR-dependent membrane depolarization. Fluorescein introduced into petioles spreads at similar rates in the wild type (WT) and the *glr3.3 glr3.6* mutant (Figure 1G). This indicated that membrane depolarizations typical of the SWP were not needed for transport of the fluorophore. Then, using fluorescein-isothiocyanate (FITC) dextrans, we determined the masses of molecules that can travel from a wounded petiole to a distal leaf. These experiments revealed that molecules with masses of at least 500 kDa were readily transported through the xylem (Figure 1H). To slow fluid movement in the transpiration stream, we shaded individual leaves. When distal leaf laminae were shaded for 3 h (Figure 1I), the velocity of propagation of fluorescein was reduced in distal leaf petioles (Figure 1J). Similarly, shading distal receiver leaves (Figure 1K) slowed the SWP in the petioles of these leaves (Figure 1L). In addition to shading treatments, and also designed to reduce transpiration, receiver leaf 13 was coated with paraffin oil (Figure S1A). Like shading, this treatment reduced SWP velocities from leaf 8 to leaf 13 (Figure S1B) without significantly affecting SWP amplitudes and durations (Figure S1C). Next, petioles were severed in a solution of the dye basic fuchsin, and sections of the plant were examined. Fuchsin was visible in the leaf 8 petiole and was detected in xylem vessels in distal leaf 13 but not in leaf 9 that does not share a direct vascular connection with leaf 8 (Figure 1M). Experiments were then designed to identify the nature of the membrane depolarization elicitors transported from a wounded leaf to a distal leaf.

An assay for Ricca's factors in *Arabidopsis*

Ricca[4] heat-killed sections of petioles of *Mimosa* leaves and showed that when the tips of these leaves were burned, elicitor substances passed through the killed petiole to elicit distal leaf movements. We recapitulated part of Ricca's procedure in *Arabidopsis* by pipetting boiling water onto petioles (Figure 2A). Plants were then incubated for 3 h in the light prior to experimentation. At this point, xylem vessel lumens in scalded tissues were visible and of similar dimensions to those from undamaged petioles (Figure 2B). When the petiole of leaf 13 was cut in a fluorescein solution, fluorescence was transported efficiently through the scalded petiole of leaf 8 (Figure 2C). Using fluorescein, we compared the velocity of mass transfer from leaf 13 to leaf 8 in the absence and presence of scalds on the leaf 8 petiole. In parallel, SWPs were examined with a similar experimental design (Figure S1D). In both cases, the velocities of mass transfer and the SWP were slightly reduced in the scalded plants (Figure S1E). When the blade of leaf 8 was crushed, the propagation of SWPs occurred even after the petiole of that leaf or the petiole of leaf 13 was scalded (Figure 2D). Finally, when the healthy petiole proximal to the heat-treated tissue was severed, SWP-like signals were detected in distal leaf 13. However, when the heat-treated tissue was severed, no surface potential changes were recorded in leaf 13 (Figure 2E). Together, these experiments established the basis of an assay for the detection of xylem-mobile mediators of membrane depolarization.

Biological activities in leaf extracts

At the outset of our experiments, we expected to find heat-stable low molecular mass elicitors of membrane potential change in leaf extracts. When the scalded regions of leaf 8 petioles were cut in fresh, undiluted, or diluted leaf extract (Figure 3A), this elicited SWP-like signals (Figure 3B). Similar depolarizations were observed at 5- and 50-fold dilutions of the fresh extract (Figures 3B and 3C). However, 50-fold diluted leaf extract that had been boiled for 5 min had no activity in the assay (Figure 3C). At this dilution, the activity of the fresh leaf extract was also destroyed by freeze-thaw cycles (Figure S2A), and it decayed in the presence of acid (Figure S2B). The activity of the diluted extract was not strongly affected by buffer concentration (Figure S2C). We used the Ricca assay and the strategy outlined in Figure 3D to purify elicitors of membrane depolarization.

Fresh leaf extract was fractionated by anion-exchange chromatography (Figure 3D), and each fraction was then assayed for its potential to elicit long-duration membrane depolarizations

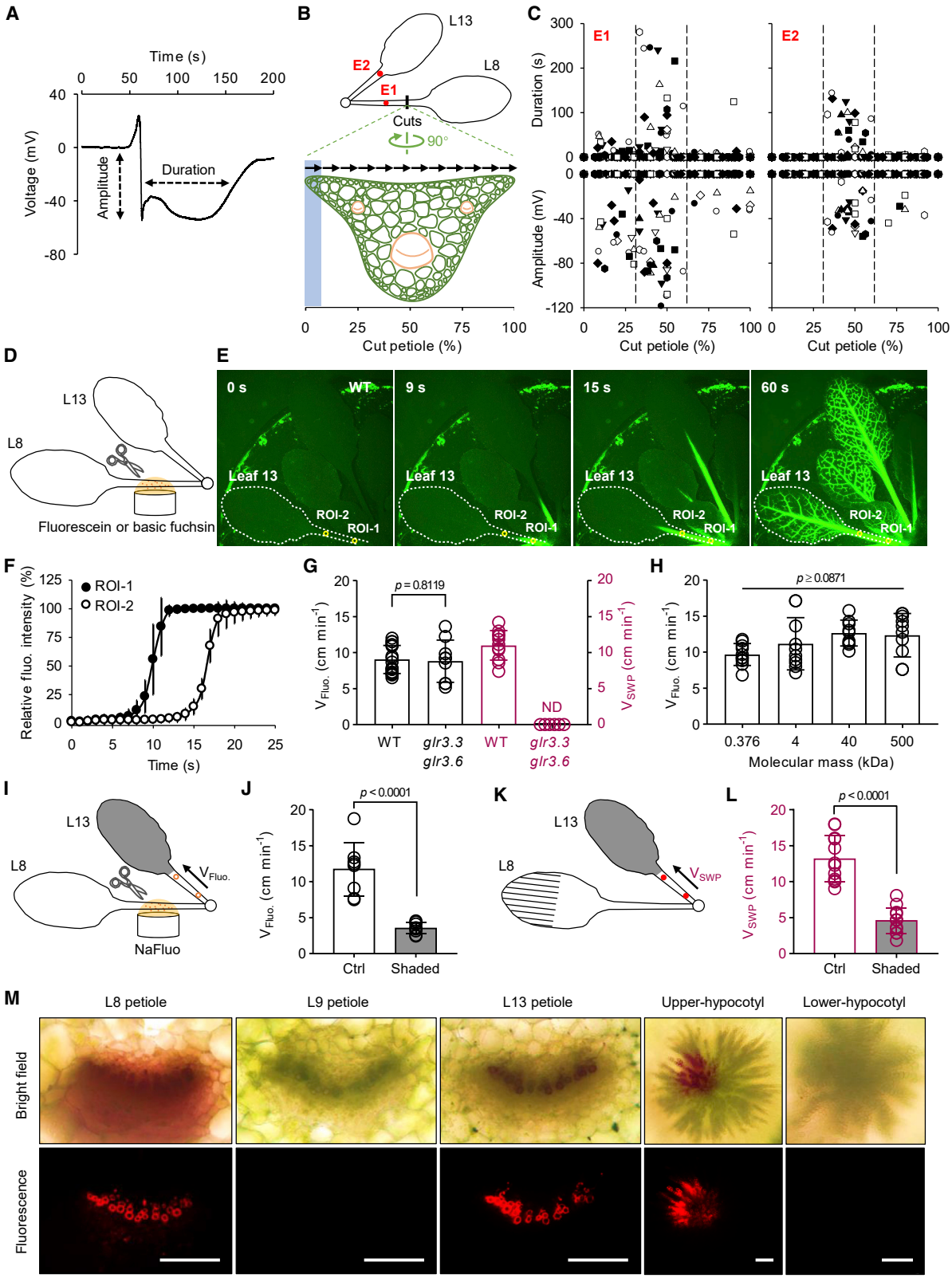

(legend on next page)

(Figure S2D). Fractions that elicited electrical activity in the bioassay were desalted and further purified using high-resolution size-exclusion chromatography. A major peak of high biological activity was recovered (Figure S2E). Gel electrophoresis revealed that the peak was enriched in proteins with masses of approximately 70 kDa (Figure S2F). Mass spectral analyses of tryptic fragments revealed 975 proteins in fractions spanning the peak of highest activity (Table S1). However, a single protein annotated as β-THIOGLUCOSIDE GLUCOHYDROLASE 1 (TGG1) accounted for an estimated 70% of peptides in the highly active fractions collected (Figure 3E). A second closely related protein, TGG2, was the third most-abundant source of peptides in these fractions, and low-abundance peptides from the related protein TGG3 were also recovered in the high-activity fractions (Figure S2G). These findings incited us to test whether TGGs were involved in leaf-to-leaf electrical signaling.

TGGs are necessary for SWP generation

Focusing on TGG1, we asked whether this protein alone could trigger activity in the Ricca assay, as described in Figure 3A. To eliminate all other plant-derived components, recombinant TGG1 was produced in insect cells[17] and purified by tandem affinity chromatography (Figures S3A–S3C). Size-exclusion chromatography (Figure S3B) followed by gel electrophoresis (Figure S3C) revealed that TGG1 in solution existed principally as monomers and dimers. TGG1 is a myrosinase enzyme that catalyzes the hydrolysis of β-thioglucosides and β-glucosides.[18] Recombinant TGG1 was catalytically active (Figure S3D), and in the Ricca assay this protein triggered strong, long-duration electrical signals typical of SWPs (Figures 4A and 4B). By contrast, the boiled protein was inactive (Figures 4A and 4B). The production of two catalytically inactive variants of the protein confirmed that TGG1 enzymatic activity was necessary for its elicitor action (Figures S4A–S4C). TGG1 displayed robust activity in the Ricca assay down to approximately 0.5 μM concentrations (Figures 4C and S4D).

Given that TGG1 was an active elicitor of long-duration membrane depolarization, we next tested whether *tgg* mutants affected SWP signaling. For initial screening of these mutants, leaf 8 of intact plants was crush wounded, and SWPs were recorded on leaf 13. While the *tgg*1, *tgg2*, and *tgg3* single mutants did not significantly affect SWPs detected in distal leaf 13, the *tgg1 tgg2* double mutant failed to produce WT-like SWPs, as did a *tgg1 tgg2 tgg3* triple mutant (Figure S5A). We then focused on the *tgg1 tgg2* double mutant. When leaf 8 of the WT is wounded, leaf 13 receives SWP signals, whereas leaf 9 does not.[6] No SWPs were detectable in leaf 9 of the WT or *tgg1 tgg2* mutant in response to wounding leaf 8 (Figure S5B). Since the leaf 8/leaf 13 pair was used in most experiments, we tested whether the effects of studying a different leaf pair produced similar results. Leaf 7 of the WT and *tgg1 tgg2* was wounded, and SWPs were monitored on leaf 12. Surface potentials on leaf 12 of the double mutant had greatly reduced durations in comparison to the WT (Figure S5C). We confirmed that fresh leaf extracts from the *tgg1 tgg2* double mutant had low myrosinase activity, compared with extracts from the WT (Figure S5D). In order to verify that the mobility of molecules in the xylem was not impaired in *tgg1 tgg2*, we compared fluorescein mobility in the WT and in *tgg1 tgg2*. These tests (Figure S5E) revealed that the *in planta* mobility of fluorescein was similar in the double mutant compared with the WT. We next conducted experiments with leaf extracts obtained from the *tgg1 tgg2* double mutant and noted that fresh, undiluted leaf extract derived from these leaves was less active in stimulating long-duration depolarizations than the extract from the WT (Figure S5F). Further experiments were then conducted with recombinant TGG1. This protein elicited similar long-duration depolarizations in both the WT and the *tgg1 tgg2* background (Figure S5G).

Herbivore-induced SWPs are highly attenuated in *tgg1 tgg2* double mutants

To test whether *tgg1 tgg2* affected electrical signaling in response to herbivory, we caged larvae of the lepidopteran *Pieris brassicae* on leaf 8 of *tgg1 tgg2* and monitored SWPs on leaf 13 (Figure 4D). Relative to the WT that showed archetypal electrical signals in leaf 13, 57% of double mutant plants showed no SWPs

Figure 1. Xylem-transmitted Ricca's factors mediate electrical signaling upon wounding

(A) Typical slow wave potential (SWP) measured on the petiole of leaf 13 after wounding leaf 8.

(B) Experimental design for step cutting and electrical signal detection. Intact plants were used for test; only schematic of leaf 8 (L8) and leaf 13 (L13) are shown here. Surface electrodes E1 and E2 indicated as red dots. The schematic petiole section shows the midvein and secondary veins (brown); arrows and blue shading indicate successive cuts. Cuts were made at 100-μm intervals.

(C) Step cut-induced electrical signals in wild-type (WT) plants. Left, recordings from E1 on petiole 8 and right, recordings from E2 on petiole 13. Regions between dashed lines indicate long-duration depolarizations. The different symbols represent individual plants. 6 ± 1 cuts of the leaf 8 petiole were required to initiate SWPs in leaf 13; 12 ± 2 cuts were required to cut off the petiole (n = 19).

(D) Experimental design for fluorescein (1 mg mL^{-1}) and basic fuchsin (0.01%, w/v) loading by cutting petiole 8 in solution.

(E) Propagation of sodium fluorescein (NaFluo) in a WT plant. Fluorescence from two regions of interest (ROIs) in petiole 13 (open circles, 50 pixels) was analyzed.

(F) NaFluo propagation in petiole 13 (n = 8).

(G) Velocity of NaFluo propagation in petiole 13 of the WT and *glr3.3 glr3.6* (shown in black; n = 9–17); and velocity of SWPs in petiole 13 after crush wounding leaf 8 (shown in maroon; n = 6–11; ND, not detected).

(H) Velocity of NaFluo and fluorescein-isothiocyanate dextran (FITC-dextran) propagation in distal petiole 13 of WT plants (n = 9–10).

(I) Experimental design for NaFluo loading with distal leaf shaded. NaFluo was supplied 3 h after shading leaf 13 with aluminum foil.

(J) Velocity of NaFluo propagation in petiole of shaded leaf 13 (n = 8).

(K) Experimental design for wound-induced SWP propagation in shaded distal leaf. Leaf 8 was wounded 3 h after shading leaf 13 with aluminum foil.

(L) Velocity of SWP propagation in petiole of shaded leaf 13 (n = 12).

(M) Transverse sections 4 h after basic fuchsin feeding. Note that basic fuchsin does not appear to be transported downward toward the roots. Scale bars, 100 μm. Data are means ± SD; unpaired two-tailed Student's t test for (G), (J), and (L); one-way ANOVA followed by Tukey's test for (H).

See also Figure S1.

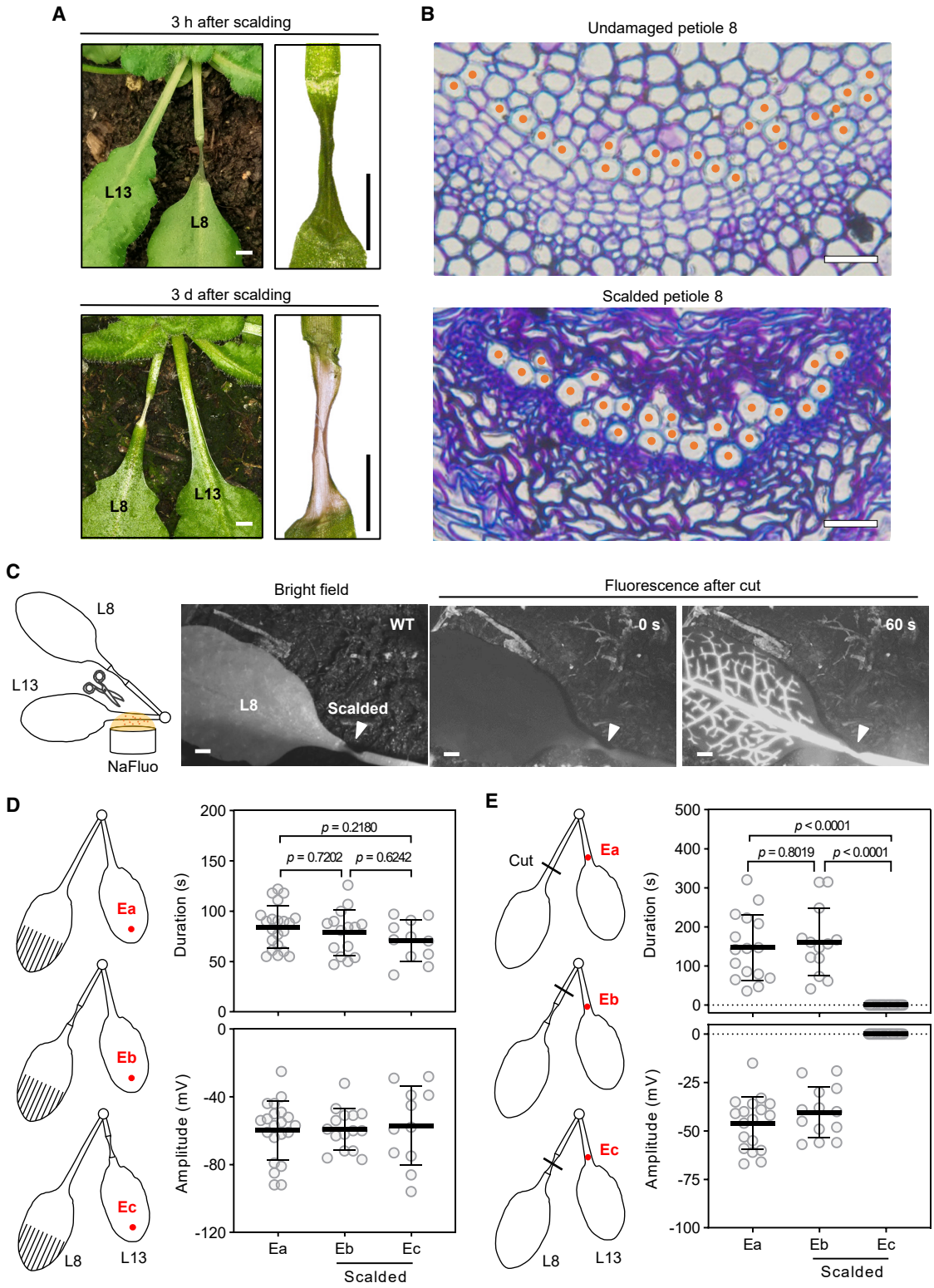

Figure 2. Ricca's factors are released by live tissues

(A) WT plants after petiole scalding. Left, petioles 3 h (upper) or 3 days (lower) after scalding; right, higher magnification images of scalded petiole 8 (all scale bars, 2 mm).

(legend continued on next page)

in leaf 13 and, in the other 43%, the repolarization phase of the SWP was strongly attenuated (Figures 4E and 4F). SWPs activate jasmonate-dependent defense gene expression in leaves distal to wounds, and the expression of the *JASMONATE ZIM-DOMAIN 10* (*JAZ10*) gene provides a marker for these responses.[6] When we caged insects on leaf 8, they failed to strongly activate *JAZ10* expression in leaf 13 of the *tgg1 tgg2* double mutant (Figure 4G). Therefore, during insect attack, TGG1 and TGG2 are necessary for the activation of *JAZ10* expression in leaves distal to feeding sites.

Response of *glutamate receptor-like* mutants to TGG1 and to glutamate

Having established the importance of TGG1 and TGG2 in SWP signaling, we then investigated potential genetic interactions between the TGGs and two GLR genes, *GLR3.3* and *GLR3.6*, that are essential for *Arabidopsis* SWP signaling.[6] In a first series of experiments, recombinant TGG1 protein was fed into petioles of the WT, the *glr3.3* and *glr3.6* single mutants, and the *glr3.3 glr3.6* double mutant. In response to TGG1 introduction into the xylem, the *glr3.3* mutant produced short-duration, high-amplitude depolarizations. However, TGG1-induced depolarizations were absent in the *glr3.6* single mutant and in the *glr3.3 glr3.6* double mutant (Figure 4H).

The amino acid L-glutamate (L-Glu), a potential activating ligand for GLRs, is implicated in leaf-to-leaf wound signaling.[10] We used the Ricca assay to compare the activity of glutamate with that of TGG1 in both the WT and in *tgg1 tgg2*. Glutamate-induced electrical activity was similar in both backgrounds (Figure S5H). However, when we fed glutamate into *glr* mutants, we found that *glr3.3* strongly attenuated surface potentials (Figure 4I). In *glr3.6* the rapid depolarization phase was similar to that of the WT, but the duration of the repolarization phase was increased relative to the WT. These experiments indicate that glutamate and TGG1 act through different mechanisms to elicit changes in membrane potential.

In order to investigate potential genetic interactions of *TGG*s and *GLR*s, we produced *tgg1 tgg2 glr3.3* and *tgg1 tgg2 glr3.6* triple mutants. These plants were then compared with the WT, *tgg1 tgg2*, and the *glr3.3* and *glr3.6* single mutants for their ability to produce SWPs (Figure 4J). As expected from previous results, both the *tgg1 tgg2* and the *glr3.3* mutants reduced SWP durations. When the *tgg1 tgg2 glr3.3* triple mutants were crush wounded, they showed a strong reduction in both the amplitudes and durations of the SWP. In the case of *tgg1 tgg2 glr3.6*, the SWP duration was attenuated strongly and to the same extent as in the *glr3.6* single mutant (Figure 4J). Both the xylem and phloem participate in SWP propagation.[9] Using living aphids as sieve element-specific electrodes,[19] we probed the electrical activity of the phloem in response to wounding. These experiments (Figures 5A, 5B, and S6) revealed that instead of producing signals typical of the WT, *tgg1 tgg2* mutants either displayed no signals (6/8 plants) or the signals were attenuated (2/8 plants).

TGGs induce cytosolic Ca^{2+} transients

Wounding causes GLR-dependent increases in cytosolic Ca^{2+} levels in injured leaves and in leaves distal to wounds.[9,10] Like the SWP, leaf-to-leaf Ca^{2+} transients could propagate through the scalded petiole with slightly reduced apparent velocities relative to those in unscalded plants (Figures S7A and S7B). Since recombinant TGG1 triggered SWPs in WT plants (Figures 4A and 4B), we tested whether this protein could also trigger cytosolic Ca^{2+} transients in the WT. When TGG1 was fed into the WT using the Ricca assay, the protein elicited transient cytosolic Ca^{2+} increases in distal leaves (Figure 5C). To assess the impact of the *tgg1 tgg2* double mutant on wound-response cytosolic Ca^{2+} levels, the intensometric Ca^{2+} reporter GCaMP3 was introgressed into this mutant. These plants were then wounded on leaf 8, and SWPs and cytosolic Ca^{2+} were monitored in leaf 13 (Figures 5D–5F). The two *tgg* double mutant/GCaMP3 lines tested displayed similar SWPs with durations of 29% and 25% of those seen in the WT. These lines were then compared with the WT for their ability to produce wound-response cytosolic Ca^{2+} transients. Peak post-wounding Ca^{2+} transients in two *tgg1tgg2*/GCaMP3 lines were 13% and 20.5% of peak levels in the WT (Figure 5F). Since *glr* mutants attenuate electrical signaling induced by exogenous TGG1 (Figure 4H) or glutamate (Figure 4I), the ability of these elicitors to trigger Ca^{2+} transients in *glr3.3* and *glr3.6* backgrounds was investigated. TGG1-induced cytosolic Ca^{2+} transients were abolished in *glr3.6* single mutants and in the *glr3.3 glr3.6* double mutant. In *glr3.3* plants, the Ca^{2+} transient was greatly reduced (Figure S7C). Consistent with Toyota et al.,[10] exogenous glutamate fed into petioles triggered large cytosolic Ca^{2+} increases in the WT but not in *glr3.3 glr3.6*. We found that glutamate-induced cytosolic Ca^{2+} transients were completely abolished in the *glr3.3* single mutant and in the *glr3.3 glr3.6* double mutant. However, glutamate-induced Ca^{2+} transients were similar in the *glr3.6* single mutant and the WT (Figure S7D).

Aliphatic GSL breakdown in veins is necessary for SWP generation

Specialized defense molecules called glucosinolates (GSLs) are among the natural substrates for TGGs.[20] Since the catalytic activity of TGG1 was required for its SWP-inducing activity, we

(B) Representative transverse sections of an undamaged WT petiole and a petiole from the WT 3 h after scalding. In both cases, the petiole of leaf 8 was used. Xylem vessels are indicated with orange dots (scale bars, 20 μm).
(C) Propagation of NaFluo through a previously scalded petiole of WT plant. Representative images of NaFluo in distal leaf 13 (scale bars, 2 mm). NaFluo was applied at a concentration of 1 mg mL^{-1}.
(D) SWPs can traverse scalded tissues of WT plants. Left, experimental designs for petiole scalding, crush wounding, and SWP recording with surface electrodes (red dots) 5 mm from the tip of leaf 13; right, SWPs recorded after crush wounding leaf 8 (n = 11–21).
(E) Cut-induced SWPs in distal leaf 13 of WT plants. Left, experimental design for petiole scalding, cutting with scalpel blade, and SWP recording with surface electrodes (red dots) on petiole 13; right, SWPs recorded after cutting (n = 11–26). For (B)–(E), plants were used 3 h after scalding. Data are means ± SD; one-way ANOVA followed by Tukey's test.
See also Figure S1.

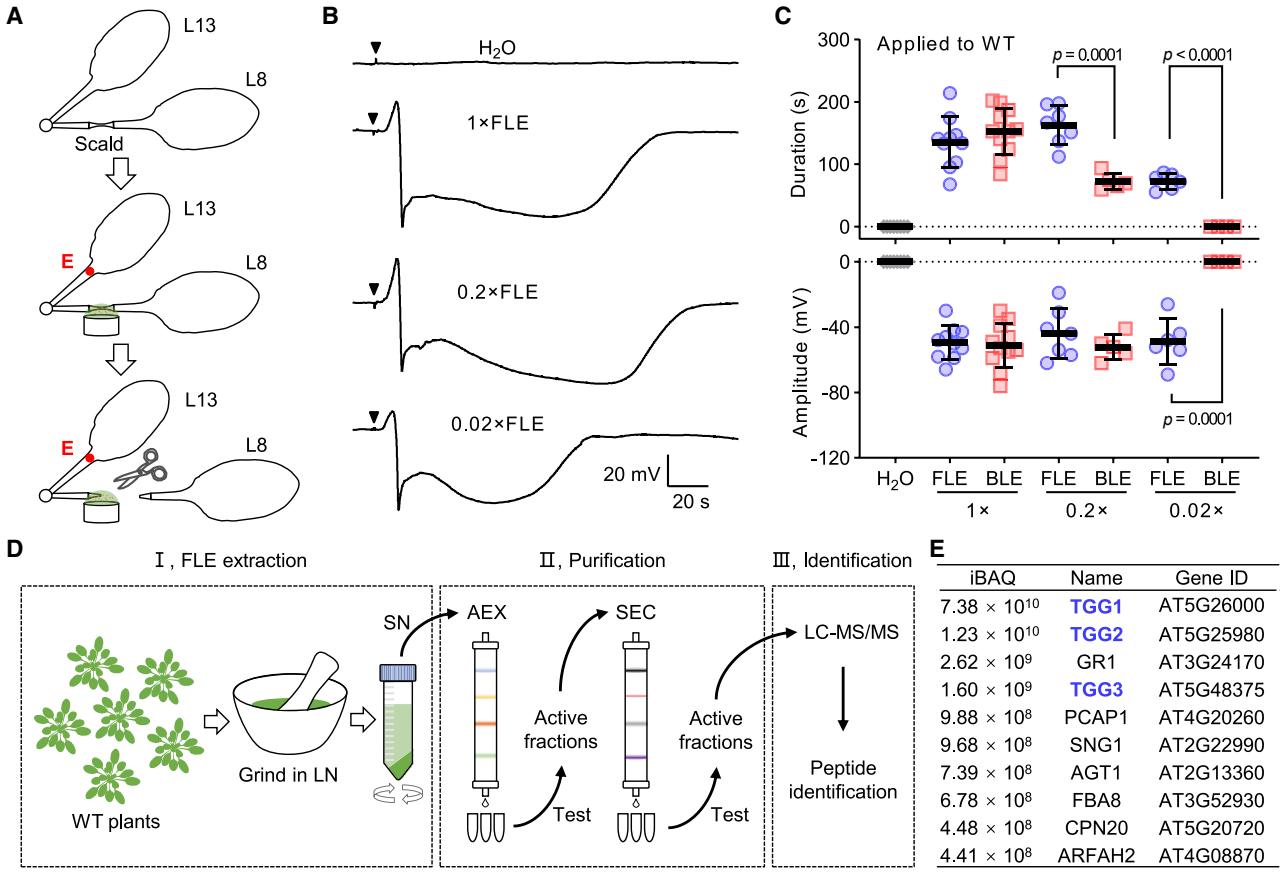

E

iBAQ	Name	Gene ID
7.38×10^{10}	TGG1	AT5G26000
1.23×10^{10}	TGG2	AT5G25980
2.62×10^{9}	GR1	AT3G24170
1.60×10^{9}	TGG3	AT5G48375
9.88×10^{8}	PCAP1	AT4G20260
9.68×10^{8}	SNG1	AT2G22990
7.39×10^{8}	AGT1	AT2G13360
6.78×10^{8}	FBA8	AT3G52930
4.48×10^{8}	CPN20	AT5G20720
4.41×10^{8}	ARFAH2	AT4G08870

Figure 3. Purification of Ricca's factors from *Arabidopsis*

(A) Ricca assay setup. Experimental design for petiole scalding, solution application, and electrical signal detection (red dots represent surface electrodes).

(B) Typical SWPs measured on the petiole of leaf 13 in WT plants after solution application. Inverted black triangles indicate the time point of cuts.

(C) Fresh undiluted leaf extract (FLE)- and boiled undiluted leaf extract (BLE)-induced SWPs in WT plants (means ± SD; n = 4–11; unpaired two-tailed Student's t test). In (B) and (C), leaf extract from WT plants were used.

(D) Procedure for Ricca's factor identification. LN, liquid nitrogen; SN, supernatant; AEX, anion-exchange chromatography; SEC, size-exclusion chromatography; LC-MS/MS, liquid chromatography-tandem mass spectrometry.

(E) Ranking of the highest abundance peptides in highly active fractions from mass spectrometry. iBAQ, intensity-based absolute quantification. Note the high relative abundance of peptides from TGG1 and the presence of TGG2 and TGG3 shown in blue.

See also Figure S2 and Table S1.

turned our attention to these metabolites. If GSL hydrolysis contributes to SWP elicitation in wounded plants, this process must occur rapidly in the veins of leaves distal to damage sites. It takes less than 90 s for an SWP initiated by wounding leaf 8 to reach an electrode placed on the petiole of leaf 13.[6,14] Therefore, we chose a 120-s time frame between wounding leaf 8 and extracting primary veins from distal leaf 13 (Figure 6A). Using HPLC-MS metabolite profiling, intact GSLs and their isothiocyanate (ITC) breakdown products were then analyzed. As a control, *tgg1 tgg2* plants, which have reduced capacities to hydrolyze GSLs,[21] were examined in parallel. These analyses revealed no significant differences in the levels of intact GSLs in veins from undamaged and wounded WT plants (Figure S8A). However, significantly more ITC breakdown products derived from aliphatic GSLs were found in wounded WT veins than in veins extracted from undamaged WT plants (Figure 6B). These results revealed that aliphatic GSL breakdown in the veins of distal leaf 13 occurs sufficiently rapidly to contribute to SWP production. To further explore this, we again deployed the Ricca assay. Glucoraphanin is an aliphatic GSL that is known to occur in xylem vessels in undamaged WT *Arabidopsis* leaves.[22] This compound was among those broken down rapidly in the distal leaf veins of the wounded WT (Figure 6B). Glucoraphanin supplied to petioles of WT plants in the absence of TGG1 did not trigger membrane depolarization, but adding TGG1 to glucoraphanin triggered SWPs similar to those produced by TGG1 alone (Figures 6C and 6D). These results are consistent with a model in which TGG1 encounters endogenous pools of aliphatic GSLs as it travels through the xylem, and this leads to SWP elicitation. We tested this possibility using genetic approaches.

The *myb28 myb29* double mutant lacks the ability to produce aliphatic GSLs.[23] Remarkably, TGG1 applied in the Ricca assay

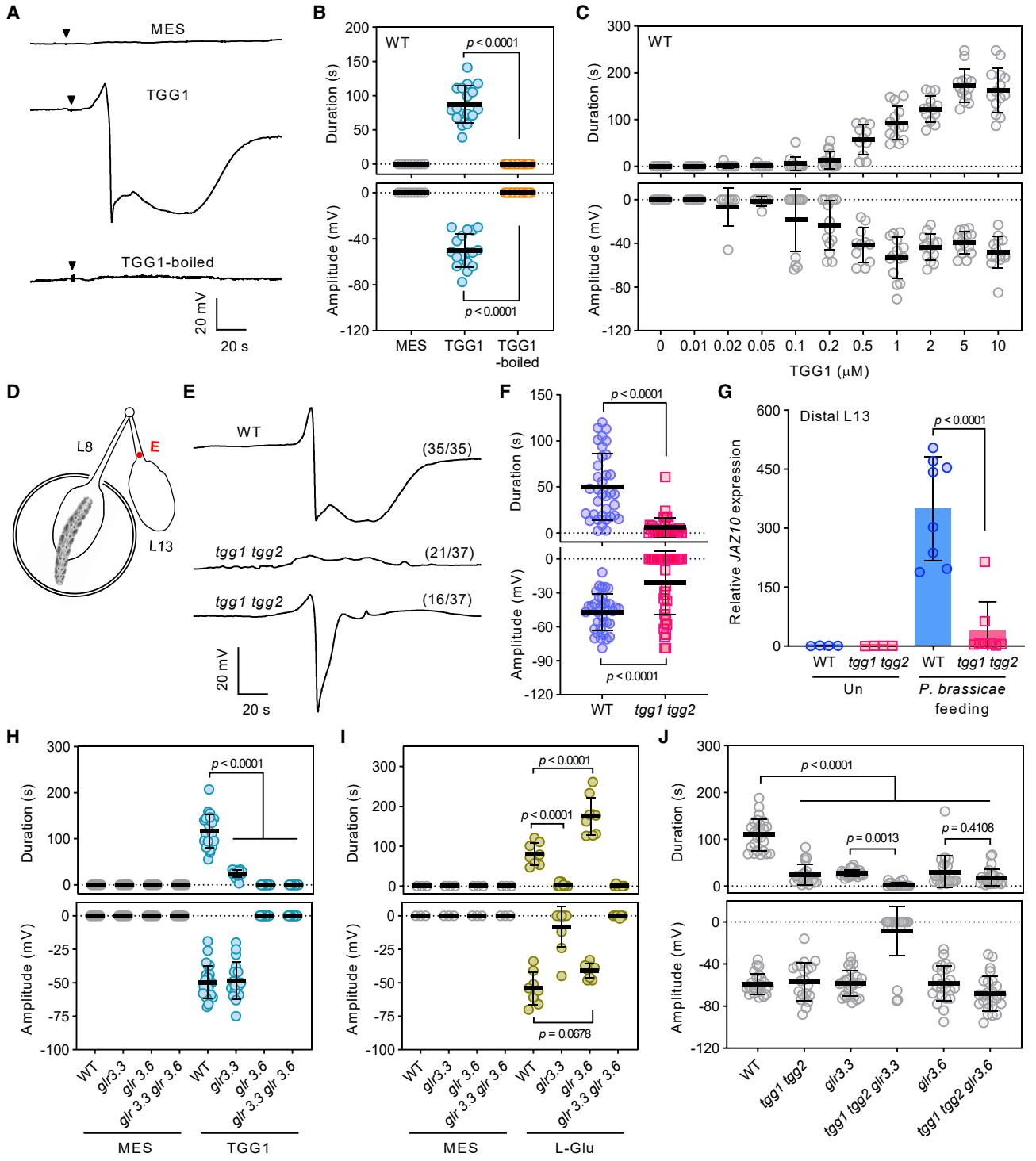

Figure 4. Myrosinases TGG1/2 mediate long-distance electrical signaling

(A and B) SWPs induced by 1 μM recombinant TGG1 protein in WT plants (n = 9–17). MES, 50 mM MES, pH 6.0 with Tris as negative control. Boiling was for 5 min. Inverted black triangles indicate the time point of cuts.

(C) Dose-response for TGG1 activity at different concentrations in WT plants (n = 4–14).

(D) Experimental design for *Pieris brassicae* larvae feeding-induced electrical signal detection (red dot, surface electrode).

(E and F) *P. brassicae* feeding-induced SWPs in *tgg1 tgg2*. Data in parentheses in (E) represent the number of typical recordings/total recordings.

(G) *JAZ10* expression analyses in distal leaf 13 1 h after *P. brassicae* feeding (n = 4–8). Un, undamaged plants.

(legend continued on next page)

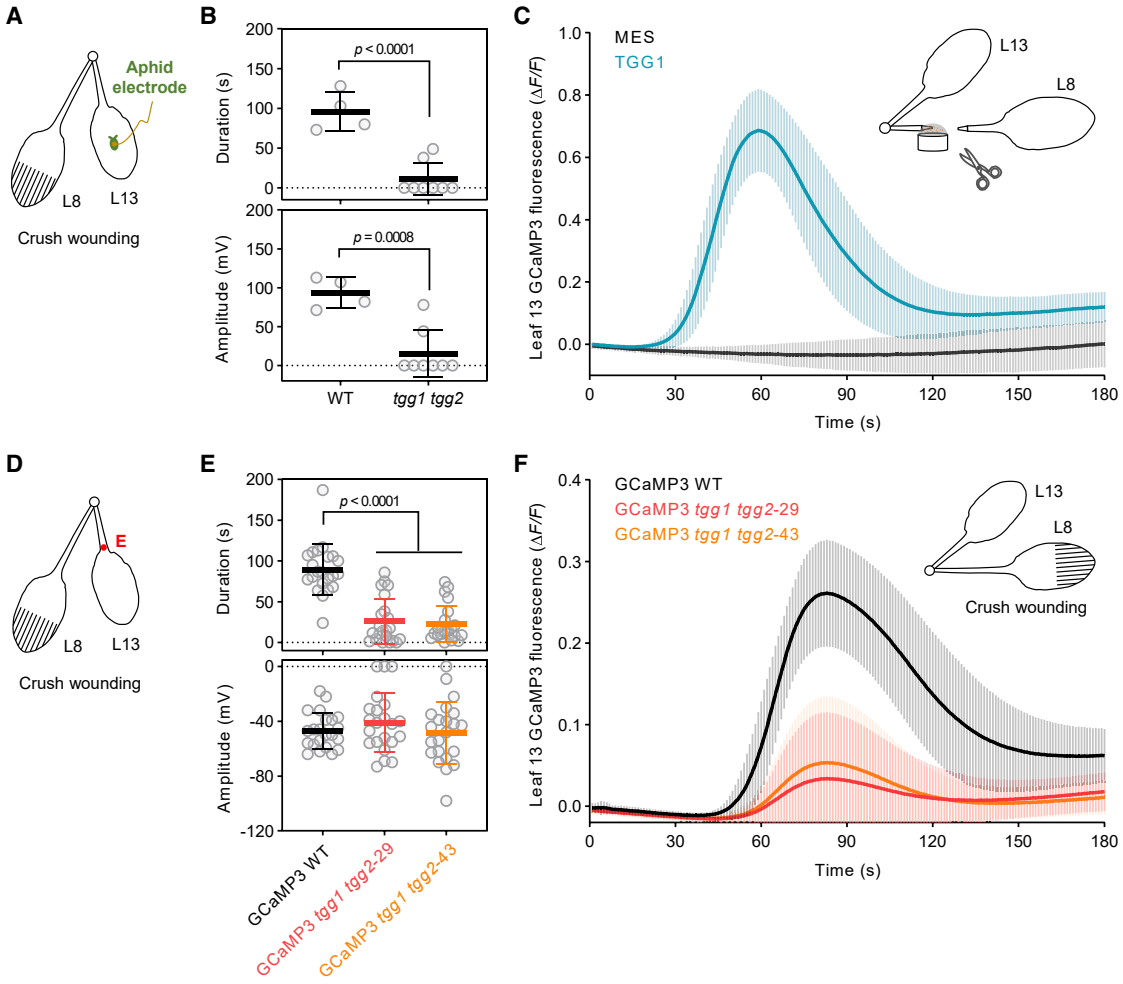

Figure 5. TGG1/2-dependent phloem electrical signals and cytosolic Ca^{2+} transients induced by mechanical wounding

(A) Experimental design for electrical penetration graph (EPG) recordings from sieve elements. Green indicates the aphid electrode.

(B) EPG recordings from *tgg1 tgg2* (means ± SD; n = 4–8; unpaired two-tailed Student's t test).

(C) Recombinant TGG1-induced cytosolic Ca^{2+} transients in GCaMP3-expressing WT plants (means ± SD; n = 5–10). Inset, experimental design for solution loading. 1 μM recombinant TGG1 protein in MES buffer was fed through the scalded petiole of leaf 8, and GCaMP3 fluorescence from leaf 13 (petiole and lamina) was analyzed. MES, 50 mM MES, pH 6.0 with Tris as negative control.

(D) Experimental design for crush wounding and electrical signal detection (red dot, surface electrode).

(E) Crush wound-induced SWPs in GCaMP3-expressing WT and *tgg1 tgg2* plants (means ± SD; n = 22; one-way ANOVA followed by Tukey's test).

(F) Crush wound-induced cytosolic Ca^{2+} transients in the WT and *tgg1 tgg2* plants (means ± SD; n = 20–23). Inset, experimental design for crush wounding leaf 8 and GCaMP3 fluorescence detection from leaf 13 (petiole and lamina).

Envelopes in (C) and (F) represent standard deviation.

See also Figures S6 and S7.

failed to elicit membrane depolarizations in *myb28 myb29* unless the protein was supplied to the plant in the presence of the aliphatic GSL glucoraphanin (Figure 6D). Three structurally different GSLs were then tested in this assay. In each case, the GSL in the presence of TGG1 elicited SWPs in the *myb28 myb29* mutant (Figures S8B–S8E). Therefore, a variety of GSLs are likely to serve as *in vivo* precursors for SWP-eliciting activities. Focusing on glucoraphanin, we fed this compound

(H) TGG1 (1 μM)-induced SWPs in *glr* mutants (n = 9–23).

(I) L-Glu-induced SWPs in *glr* mutants (n = 3–10). 5 mM L-glutamic acid in 50 mM MES, pH 6.0 with Tris was applied.

(J) Crush wounding-induced SWP in different genotypes (n = 21–26). Leaf 8 was crush wounded, and electrical signals in petiole 13 were recorded.

In (A), (B), (C), and (H), TGG1 was diluted with 50 mM MES, pH 6.0 with Tris. TGG1 protein or L-Glu was applied from leaf 8, and electrical signals were measured on the petiole of leaf 13. Data are means ± SD; unpaired two-tailed Student's t test for (B), (F), and (G); one-way ANOVA followed by Tukey's test for (H)–(J).

See also Figures S3, S4, S5, and Table S2.

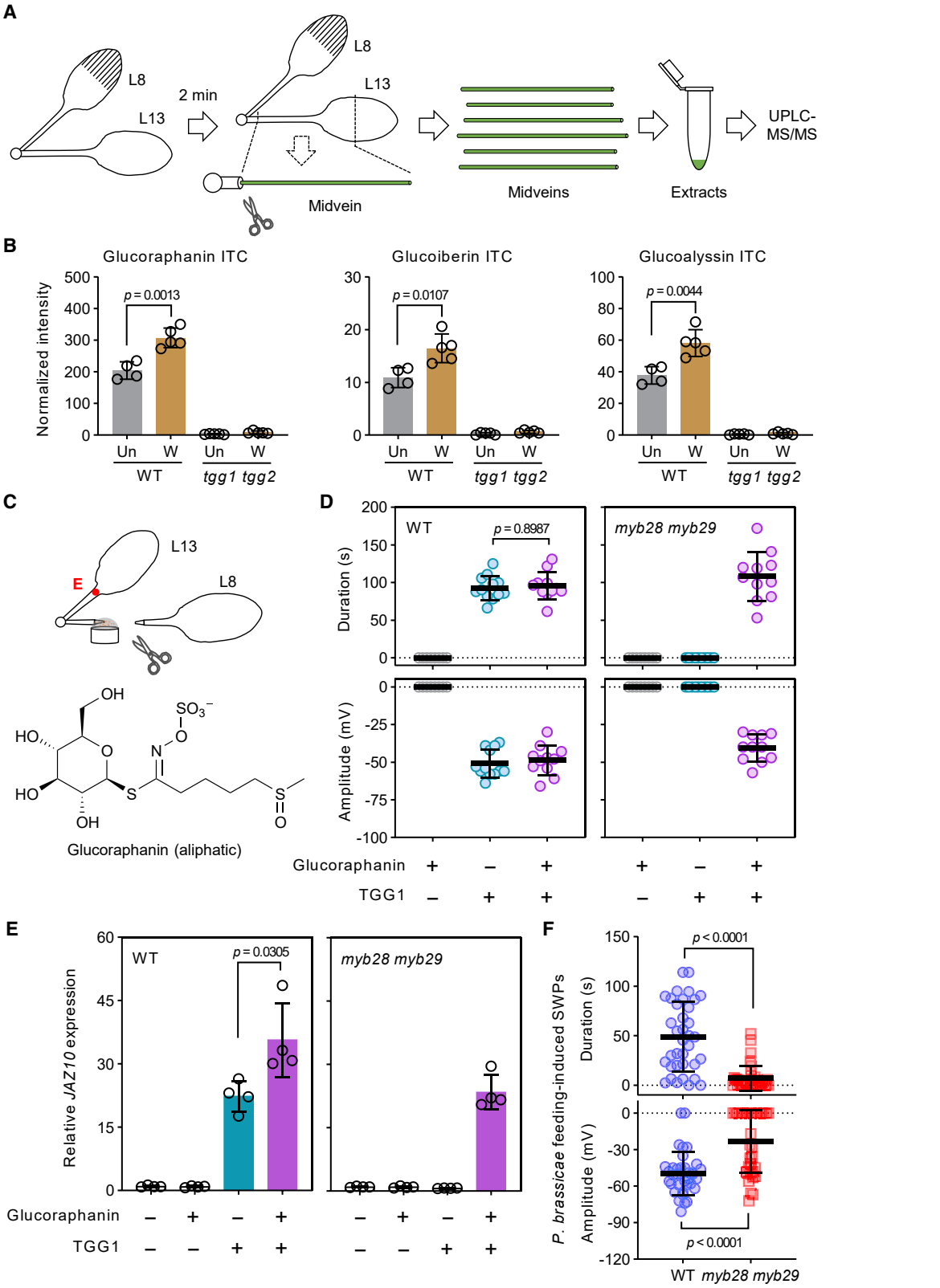

(legend on next page)

together with TGG1 into *myb28 myb29* leaves using the Ricca assay. We estimated the half-maximum activity of glucoraphanin to be approximately 20 μM (Figures S8F and S8G).

Related to these experiments we investigated TGG1-induced *JAZ10* expression in the WT and in *myb28 myb29*. We found that glucoraphanin supplied to WT plants did not induce expression of the jasmonate signaling marker gene *JAZ10* (Figure 6E). However, TGG1 alone or in combination with glucoraphanin caused *JAZ10* transcript accumulation in WT plants. Only the mixture of glucoraphanin and TGG1 induced *JAZ10* transcript accumulation in the *myb28 myb29* mutant (Figure 6E). The Ricca assay can therefore be used to evaluate jasmonate pathway stimulation by exogenous elicitors. Relative to the WT, the *glucosinolate transporter 1, 2* double mutant (*gtr1 gtr2*)[24] has increased levels of GSLs in expanded leaves.[25] When *gtr1 gtr2* was wounded, it produced SWPs similar to those of the WT (Figure S8H). Our results raised the question of whether plants with reduced levels of aliphatic GSLs could produce SWPs when attacked by herbivores. Confirming a role of aliphatic GSLs in the control of membrane potential, shorter duration electrical signals occurred in the insect-damaged *myb28 myb29* plants compared with the WT (Figure 6F). Together, these findings reveal that aliphatic GSL breakdown in veins is necessary for herbivore-triggered membrane depolarization in leaves distal to wounds.

The nature of the Ricca's factor in *Arabidopsis*

A defining feature of Ricca's factors is their ability to travel over long distances from leaf to leaf.[4] We therefore tested TGG1 mobility by feeding affinity-tagged TGG1 protein into the leaf 8 petiole and then probing extracts from leaf 13 with antibodies directed against the tag (Figure 7A). TGG1 was detected in the distal leaf 13 (Figure 7B). Therefore, TGG1 is a component of the *Arabidopsis* Ricca's factor. Given that the duration of insect-elicited membrane depolarization was reduced relative to the WT in plants lacking aliphatic GSLs (Figure 6F), we examined the process of TGG-catalyzed GSL breakdown. GSL hydrolysis produces glucose and unstable aglucone intermediates (thiohydroximate-*O*-sulfonates) that decay into a variety of more stable products.[20] The *myb28 myb29* mutant with reduced levels of aliphatic GSLs (including glucoraphanin) was used to test whether stable elicitors of membrane potential change are generated by GSL breakdown. As expected, freshly mixed TGG1 and glucoraphanin introduced into the leaf 8 petiole triggered long-duration membrane depolarizations in leaf 13 of the *myb28 myb29* mutant (Figure 7C). However, when TGG1, glucoraphanin, and L-ascorbate were co-incubated at 22°C for 1 h, the elicitor activity of the mixture was lost (Figure 7C). This activity could be restored by applying fresh glucoraphanin and feeding this mixture into plants (Figure 7C). The active membrane depolarization elicitors generated by TGG1 therefore have short half-lives. Thiohydroximate-*O*-sulfonates (Figure 7D), the aglycone breakdown products of GSLs,[26] were candidates for such molecules. A method to trap these unstable sulfur-rich intermediates *in vitro* has been developed: 2,2′-dipyridyl disulfide (2-PDS) traps GSL-derived aglycones *in vitro* without blocking myrosinase activity.[26] Here, we employed 2-PDS for *in vivo* chemical trapping. To do this, WT plants were supplied with TGG1 alone or with TGG1 and 2-PDS. We found that 2-PDS powerfully suppressed the long-duration TGG1-induced surface potential component (Figure 7E). Furthermore, 2-PDS in the presence of TGG1 blocked the ability of the protein to induce *JAZ10* expression (Figure 7F).

DISCUSSION

We herein confirm the Ricca[4] hypothesis that leaf-to-leaf wound-response signaling in plants requires the transport of elicitors through the xylem. Moreover, we identify the principal mobile components of the SWP-inducing Ricca's factors as thioglucosidase (TGG) proteins. The events likely to lead to SWP propagation are summarized in Figure 7G. Insects that damage vascular tissues in *Arabidopsis* leaves cause the release of TGGs from specialized myrosin cells that are embedded in the phloem parenchyma.[27,28] Our results establish a crucial role for TGGs stored in these vascular idioblasts in leaf-to-leaf electrical signaling and in the induction of wound-response cytosolic Ca^{2+} transients. Also at the wound site, a second vascular idioblast population consisting of S cells[29] releases GSLs upon rupture. TGGs released from injury sites immediately encounter these GSLs so that rapid GSL hydrolysis begins in the damaged leaf. Then, as they travel through vessels to distal leaves, the TGGs encounter further pools of aliphatic GSLs that are known to reside in the xylem in undamaged plants.[22] Along their leaf-to-leaf migration route, TGGs cleave off glucosyl moieties from GSLs to produce thiohydroximate-*O*-sulfonates. In leaves distal to wounds, these reactive aglycones are necessary to trigger the long-duration component of the SWP, large cytosolic Ca^{2+} transients, and jasmonate pathway signaling activity.

GSLs are best known as defense metabolites that can confer direct resistance against herbivores.[30] However, specialized defense metabolites, including GSLs, can have regulatory functions.[31] For example, a breakdown product of 4-methoxy-indol-3-ylmethylglucosinolate acts as a signal for pathogen-triggered callose deposition.[32] We identify a different GSL-derived

Figure 6. Aliphatic glucosinolate breakdown products induce slow wave potentials

(A) Procedure for rapid midvein extraction and metabolomic analyses. UPLC-MS/MS, ultra-performance liquid chromatography-tandem mass spectrometry.

(B) Analyses of isothiocyanates (ITCs) from aliphatic glucosinolates in midveins (n = 4–5). Un, unwounded plants; W, wounded plants.

(C) Experimental design for cutting scalded petiole 8 in glucoraphanin (10 mM) and/or TGG1 solution (1 μM) and electrical signal detection (red dot, surface electrode).

(D) TGG1 and glucoraphanin breakdown products induce slow wave potentials (SWPs; n = 8–12).

(E) *JAZ10* expression analyses in distal leaf 13. Glucoraphanin (1 mM) and/or TGG1 (1 μM) in 50 mM MES, pH 6.0 with Tris was applied to leaf 8; leaf 13 was sampled 1 h after treatment (n = 4).

(F) *P. brassicae* feeding-induced SWPs in *myb28 myb29* (n = 36). *P. brassicae* fed on leaf 8, and electrical signals were recorded in leaf 13. Data are means ± SD; unpaired two-tailed Student's t test.

See also Figure S8.

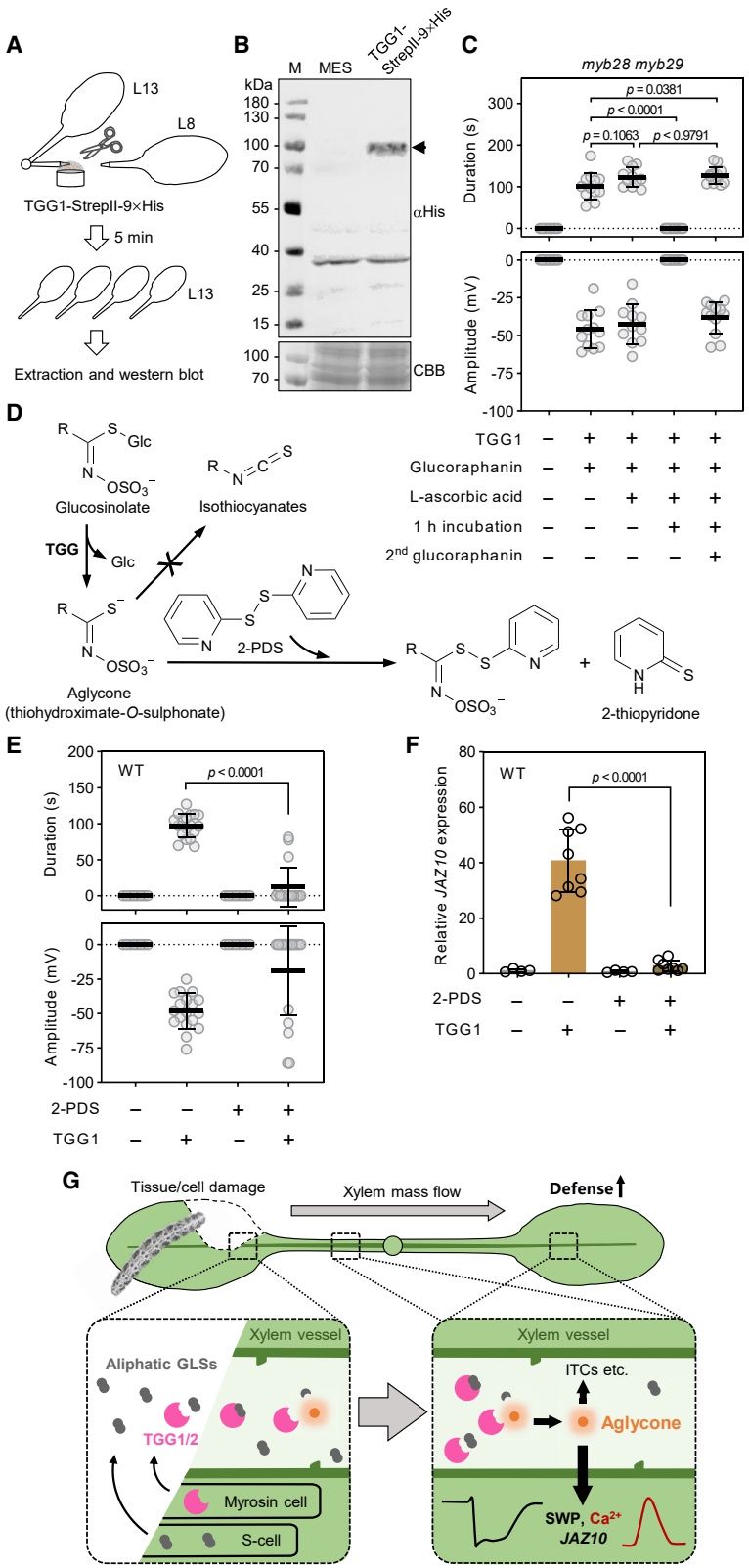

Figure 7. Ricca's factors in *Arabidopsis*

(A) Experimental design for TGG1-StrepII-9×His application and leaf sampling.

(B) Western blot analyses of TGG1-StrepII-9×His in distal leaf 13 of WT plants.

(C) Short-lived glucoraphanin breakdown products induce slow wave potentials (SWPs) in *myb28 myb29* (n = 9–12). Final concentrations of 1 μM TGG1, 1 mM glucoraphanin, and 0.3 mM L-ascorbic acid were used.

(D) TGG-mediated aglycone (thiohydroximate-*O*-sulfonate) production and trapping of aglycone with 2-PDS (2,2′-dipyridyl disulfide).

(E) Trapping of the aglycone intermediate with 2-PDS (1.5 mM) attenuates the SWPs induced by 1 μM TGG1 in WT plants (n = 8–18).

(F) *JAZ10* expression in distal leaf 13 of WT plants. 2-PDS (1.5 mM) and/or TGG1 (1 μM) in 50 mM MES, pH 6.0 with Tris was applied to leaf 8; leaf 13 was sampled 1 h after treatment (n = 4–8).

(G) Model for electrical signaling leading to Ca^{2+} transients, and defense gene activation in leaves distal to wounds. ITCs, isothiocyanates. In (C) and (E), chemicals were applied through the cut-scalded region of leaf 8 petioles. SWPs were recorded on distal leaf 13 petioles using surface electrodes. Data are means ± SD; one-way ANOVA followed by Tukey's test for (C), unpaired two-tailed Student's t test for (E) and (F).

signal function. The effects we observe are not specific to single GSLs and instead rely on reactive intermediates with different side-chain structures that can be generated from a variety of GSLs. We note that the glucoraphanin-derived aglycone has a half-life in aqueous solution of 37 s.[26] It is therefore possible that the long-duration component of the SWP is determined in part by aglycone lifetimes.

Electrical signals and Ca^{2+} transients in plants can be coupled tightly.[33,34] This is the case in the *Arabidopsis* SWP where cytosolic Ca^{2+} maxima in leaves distal to wounds occur approximately 49 s after the rapid membrane depolarization phase.[9] In the majority of cases, insect damage-induced SWPs were fully eliminated in the *tgg1 tgg2* double mutant that lacks the GSL-hydrolyzing enzymes β-THIOGLUCOSIDE GLUCOHYDROLASE 1 and 2. However, in 43% of cases, short spike-like depolarization signals remained in the distal leaves of the insect-damaged *tgg* double mutant (Figures 4E and 4F). In parallel, wound-response phloem electrical signals in leaves distal to wounds were eliminated in the majority (6/8) of *tgg1 tgg2* mutants tested. These observations were further supported by the finding that Ca^{2+} transients in *tgg1 tgg2* plants were highly attenuated but not eliminated completely, compared with those in the WT. Indeed, comparison of Figures 5E and 5F showed that the degree of reduction of SWP duration and the attenuation of maximal Ca^{2+} signal amplitudes in *tgg1 tgg2* were comparable. Together, these results suggest that there may be residual Ricca factor activity in *tgg1 tgg2*. To investigate this in more detail, we explored possible genetic interactions between TGGs, GLRs, and the amino acid glutamate.

Previous experiments revealed that *glr3.3 glr3.6* double mutants attenuate the SWP.[6] To investigate possible roles of molecules other than TGGs in SWP induction, we examined glutamate which, when applied to wounds, triggers cytosolic Ca^{2+} transients in distal leaves.[10] Moreover, wounding cotyledons with needles triggered radially spreading cytosolic Ca^{2+} waves, which were attenuated in a *glr3.3* mutant.[11] In the present work, we found that relative to the WT, the *glr3.3* mutant strongly attenuated electrical signaling and cytosolic Ca^{2+} increases when glutamate was fed into the xylem using the Ricca assay. This was not the case for *glr3.6*. This mutant produced longer-duration SWPs than the WT in response to glutamate. By contrast to glutamate treatments, feeding recombinant TGG1 into *glr* mutants revealed that both GLR3.3 and GLR3.6 were essential for membrane depolarizations triggered by this protein. This is consistent with the proposed role of both of these GLRs in SWP signaling.[6] Summarizing, we emphasize that TGGs are essential for the long-duration phase of the SWP and for the bulk of the distal wound-induced cytosolic Ca^{2+} transient.

Through genetically verifying TGGs as Ricca's factors, we resolve a long-standing enigma regarding the nature of electrical signaling elicitors in wounded plants. However, the fact that the distribution of GSLs in angiosperms is limited[30] raises the following question: is the Ricca factor signaling mechanism we describe likely to be widespread in nature? Interestingly, when Sibaoka[35] made reciprocal treatments of different plants with leaf extracts, he failed to find evidence for interspecific Ricca factor action. Sibaoka concluded that these elicitors of long-distance signaling might be "species specific." With this in mind, we note that the plant kingdom contains a great structural diversity of glucosides and that these compounds can be cleaved by enzymes related to TGGs. Ricca's factors in other plants might be produced by these variant two-component glucosidase/glucoside systems that commonly generate reactive aglucone intermediates.[36] The findings herein show that leaf-to-leaf SWP signaling in adult-phase *Arabidopsis* differs profoundly from action potential propagation along axons.[37] The long-distance translocation of high-mass protein catalysts underlies the generation of electrical signals in leaves distal to wounds. A further signaling component leading to SWP generation relies on short-lived, reactive aglycone elicitors.

Limitations of the study

The following principal limitations of the present work are apparent. First, the relevant targets of GSL-derived aglycones have yet to be identified. Thiohydroximate-*O*-sulfonates might act as ligands for regulatory proteins or ion channels. However, being unstable, the compounds might instead react with and modify the activity of such proteins. Related to this and to aglycone instability, it is not clear whether these reactive compounds can be transported between different vascular cell types in leaves distal to wounds. For example, it is conceivable that aglycones generated in vessels travel radially to the phloem to trigger membrane depolarization. Alternatively, GSL-derived aglycones might first act on xylem contact cells. However, whether this cell population in *Arabidopsis* is excitable and could thereby influence phloem electrical activity is not yet known. Finally, the impact of *glr* mutants in damaged leaves differs from that in leaves distal to injuries.[6] Related to this, we have not studied the effects of *tgg1 tgg2* mutants on signaling in the vicinity of wounds. Near damage sites, we expect that intact cells in extravascular tissues such as the epidermis, mesophyll, and bundle sheath will likely contact multiple membrane depolarizing agents.[38] Further genetic approaches will be needed to confirm the *in vivo* activities of each of these near-wound elicitors, some of which may be amino acids.

STAR★METHODS

Detailed methods are provided in the online version of this paper and include the following:

- KEY RESOURCES TABLE
- RESOURCE AVAILABILITY
  - Lead contact
  - Materials availability
  - Data and code availability
- EXPERIMENTAL MODEL AND SUBJECT DETAILS
  - Plant materials
  - Plant growth conditions
- METHOD DETAILS
  - Non-invasive electrophysiology
  - Electrical Penetration Graphs
  - Stepwise cutting of petioles
  - Fuchsin staining, fluorescein-sodium/fluorescein isothiocyanate–dextran application and data analyses

- Microscopy for petiole transversal sections
- Crush wounding
- Petiole scalding and Ricca's factor assay development
- Leaf extract preparation
- Ricca's factor purification: anion-exchange chromatography and size-exclusion chromatography
- Protein digestion for LC-MS/MS
- Liquid chromatography-tandem mass spectrometry for peptides
- MS peptide analyses
- Protein expression and purification from insect cells
- Analytical size-exclusion chromatography
- Myrosinase activity assays
- *Pieris brassicae* larvae feeding assays
- Gene expression analyses
- Calcium imaging and data analysis
- Glucosinolate analyses with extracted veins
- Western blotting

● QUANTIFICATION AND STATISTICAL ANALYSIS

SUPPLEMENTAL INFORMATION

Supplemental information can be found online at https://doi.org/10.1016/j.cell.2023.02.006.

ACKNOWLEDGMENTS

Georg Jander (Cornell) kindly provided *tgg* mutants. Tonni Grube Andersen (Max Planck Institute for Plant Breeding, Cologne, Germany) is thanked for *gtr1 gtr2* seeds.

We thank the University of Lausanne Protein Analysis Facility and in particular M. Quadroni for proteomics analyses. We are grateful to Christian Hardtke (University of Lausanne) for critical comments on the manuscript. This work was funded by Swiss National Science Foundation grants (310030_205203 and 31003A-175566) to E.E.F. and the European Research Council (ERC) grant agreement no. 716358 to J.S. The University of Lausanne also provided financial support.

AUTHOR CONTRIBUTIONS

Y.-Q.G., P.J.-S., S.T., J.W., and S.S. performed experiments; G.G. performed metabolic analyses; Y.-Q.G., P.J.-S., J.S., and E.E.F. analyzed the data; E.E.F. and Y.-Q.G. wrote the paper; and E.E.F. agrees to serve as the author responsible for contact.

DECLARATION OF INTERESTS

The authors declare no competing interests.

Received: March 22, 2022
Revised: June 26, 2022
Accepted: February 2, 2023
Published: March 3, 2023

REFERENCES

1. Stroock, A.D., Pagay, V.V., Zwieniecki, M.A., and Michele Holbrook, N.M. (2014). The physicochemical hydrodynamics of vascular plants. Annu. Rev. Fluid Mech. *46*, 615–642.
2. Alarcon, J.J., and Malone, M. (1994). Substantial hydraulic signals are triggered by leaf-biting insects in tomato. J. Exp. Bot. *45*, 953–957.
3. Dussourd, D.E. (2022). Salivary surprise: *Symmerista* caterpillars anoint petioles with red saliva after clipping leaves. PLoS One *17*, e0265490.
4. Ricca, U. (1916). Soluzione d'un problema di fisiologia: la propagazione di stimolo nellaMimosa. Nuovo G. Bot. Ital. *23*, 51–170.
5. Sambeek, J.W.V., and Pickard, B.G. (1976). Mediation of rapid electrical, metabolic, transpirational, and photosynthetic changes by factors released from wounds. I. Variation potentials and putative action potentials in intact plants. Can. J. Bot. *54*, 2642–2650.
6. Mousavi, S.A., Chauvin, A., Pascaud, F., Kellenberger, S., and Farmer, E.E. (2013). Glutamatereceptor-like genes mediate leaf-to-leaf wound signalling. Nature *500*, 422–426.
7. Cuin, T.A., Dreyer, I., and Michard, E. (2018). The role of potassium channels in *Arabidopsis thaliana* long distance electrical signalling: AKT2 modulates tissue excitability while GORK shapes action potentials. Int. J. Mol. Sci. *19*, 926.
8. Moe-Lange, J., Gappel, N.M., Machado, M., Wudick, M.M., Sies, C.S.A., Schott-Verdugo, S.N., Bonus, M., Mishra, S., Hartwig, T., Bezrutczyk, M., et al. (2021). Interdependence of a mechanosensitive anion channel and glutamate receptors in distal wound signaling. Sci. Adv. *7*, eabg4298.
9. Nguyen, C.T., Kurenda, A., Stolz, S., Chételat, A., and Farmer, E.E. (2018). Identification of cell populations necessary for leaf-to-leaf electrical signaling in a wounded plant. Proc. Natl. Acad. Sci. USA *115*, 10178–10183.
10. Toyota, M., Spencer, D., Sawai-Toyota, S., Jiaqi, W., Zhang, T., Koo, A.J., Howe, G.A., and Gilroy, S. (2018). Glutamate triggers long-distance, calcium-based plant defense signaling. Science *361*, 1112–1115.
11. Bellandi, A., Papp, D., Breakspear, A., Joyce, J., Johnston, M.G., de Keijzer, J., Raven, E.C., Ohtsu, M., Vincent, T.R., Miller, A.J., et al. (2022). Diffusion and bulk flow of amino acids mediate calcium waves in plants. Sci. Adv. *8*, eabo6693.
12. Shao, Q., Gao, Q., Lhamo, D., Zhang, H., and Luan, S. (2020). Two glutamate-and pH-regulated Ca^{2+} channels are required for systemic wound signaling in *Arabidopsis*. Sci. Signal. *13*, eaba1453.
13. Farmer, E.E., Gao, Y.Q., Lenzoni, G., Wolfender, J.L., and Wu, Q. (2020). Wound-and mechanostimulated electrical signals control hormone responses. New Phytol. *227*, 1037–1050.
14. Kurenda, A., Nguyen, C.T., Chételat, A., Stolz, S., and Farmer, E.E. (2019). Insect-damaged *Arabidopsis* moves like wounded *Mimosa pudica*. Proc. Natl. Acad. Sci. USA *116*, 26066–26071.
15. Kumari, A., Chételat, A., Nguyen, C.T., and Farmer, E.E. (2019). *Arabidopsis*H^+-ATPase AHA1 controls slow wave potential duration and wound-response jasmonate pathway activation. Proc. Natl. Acad. Sci. USA *116*, 20226–20231.
16. Evans, M.J., and Morris, R.J. (2017). Chemical agents transported by xylem mass flow propagate variation potentials. Plant J *91*, 1029–1037.
17. Moussu, S., Broyart, C., Santos-Fernandez, G., Augustin, S., Wehrle, S., Grossniklaus, U., and Santiago, J. (2020). Structural basis for recognition of RALF peptides by LRX proteins during pollen tube growth. Proc. Natl. Acad. Sci. USA *117*, 7494–7503.
18. Rask, L., Andréasson, E., Ekbom, B., Eriksson, S., Pontoppidan, B., and Meijer, J. (2000). Myrosinase: gene family evolution and herbivore defense in *Brassicaceae*. Plant Mol. Biol. *42*, 93–113.
19. Salvador-Recatalà, V., Tjallingii, W.F., and Farmer, E.E. (2014). Real-time, in vivo intracellular recordings of caterpillar-induced depolarization waves in sieve elements using aphid electrodes. New Phytol. *203*, 674–684.
20. Blažević, I., Montaut, S., Burčul, F., Olsen, C.E., Burow, M., Rollin, P., and Agerbirk, N. (2020). Glucosinolate structural diversity, identification, chemical synthesis and metabolism in plants. Phytochemistry *169*, 112100.
21. Barth, C., and Jander, G. (2006). *Arabidopsis* myrosinases TGG1 and TGG2 have redundant function in glucosinolate breakdown and insect defense. Plant J. *46*, 549–562.
22. Madsen, S.R., Olsen, C.E., Nour-Eldin, H.H., and Halkier, B.A. (2014). Elucidating the role of transport processes in leaf glucosinolate distribution. Plant Physiol. *166*, 1450–1462.

23. Sønderby, I.E., Hansen, B.G., Bjarnholt, N., Ticconi, C., Halkier, B.A., and Kliebenstein, D.J. (2007). A systems biology approach identifies a R2R3 MYB gene subfamily with distinct and overlapping functions in regulation of aliphatic glucosinolates. PLoS One *2*, e1322.

24. Nour-Eldin, H.H., Andersen, T.G., Burow, M., Madsen, S.R., Jørgensen, M.E., Olsen, C.E., Dreyer, I., Hedrich, R., Geiger, D., and Halkier, B.A. (2012). NRT/PTR transporters are essential for translocation of glucosinolate defence compounds to seeds. Nature *488*, 531–534.

25. Hunziker, P., Lambertz, S.K., Weber, K., Crocoll, C., Halkier, B.A., and Schulz, A. (2021). Herbivore feeding preference corroborates optimal defense theory for specialized metabolites within plants. Proc. Natl. Acad. Sci. USA *118*. e2111977118.

26. Mocniak, L.E., Elkin, K., and Bollinger, J.M., Jr. (2020). Lifetimes of the aglycone substrates of specifier proteins, the autonomous iron enzymes that dictate the products of the glucosinolate-myrosinase defense system in *Brassica* plants. Biochemistry *59*, 2432–2441.

27. Andréasson, E., Bolt Jørgensen, L.B., Höglund, A.S., Rask, L., and Meijer, J. (2001). Different myrosinase and idioblast distribution in *Arabidopsis* and *Brassica napus*. Plant Physiol. *127*, 1750–1763.

28. Shirakawa, M., and Hara-Nishimura, I. (2018). Specialized vacuoles of myrosin cells: chemical defense strategy in *Brassicales* plants. Plant Cell Physiol. *59*, 1309–1316.

29. Koroleva, O.A., Gibson, T.M., Cramer, R., and Stain, C. (2010). Glucosinolate-accumulating S-cells in Arabidopsis leaves and flower stalks undergo programmed cell death at early stages of differentiation. Plant J. *64*, 456–469.

30. Halkier, B.A., and Gershenzon, J. (2006). Biology and biochemistry of glucosinolates. Annu. Rev. Plant Biol. *57*, 303–333.

31. Erb, M., and Kliebenstein, D.J. (2020). Plant secondary metabolites as defenses, regulators, and primary metabolites: the blurred functional trichotomy. Plant Physiol. *184*, 39–52.

32. Clay, N.K., Adio, A.M., Denoux, C., Jander, G., and Ausubel, F.M. (2009). Glucosinolate metabolites required for an *Arabidopsis* innate immune response. Science *323*, 95–101.

33. Hagihara, T., Mano, H., Miura, T., Hasebe, M., and Toyota, M. (2022). Calcium-mediated rapid movements defend against herbivorous insects in *Mimosa pudica*. Nat.Commun. *13*, 6412.

34. Scherzer, S., Böhm, J., Huang, S., Iosip, A.L., Kreuzer, I., Becker, D., Heckmann, M., Al-Rasheid, K.A.S., Dreyer, I., and Hedrich, R. (2022). A unique inventory of ion transporters poises the Venus flytrap to fast-propagating action potentials and calcium waves. Curr. Biol. *32*. 4255.e5-4263.e5.

35. Sibaoka, T. (1997). Application of leaf extract causes repetitive action potentials in *Biophytum sensitivum*. J. Plant Res. *110*, 485–487.

36. Morant, A.V., Jørgensen, K., Jørgensen, C., Paquette, S.M., Sánchez-Pérez, R., Møller, B.L., and Bak, S. (2008). β-glucosidases as detonators of plant chemical defense. Phytochemistry *69*, 1795–1813.

37. Rama, S., Zbili, M., and Debanne, D. (2018). Signal propagation along the axon. Curr. Opin. Neurobiol. *51*, 37–44.

38. Gao, Y.Q., and Farmer, E.E. (2023). Osmoelectric siphon models for signal and water dispersal in wounded plants. J. Exp. Bot. *74*, 1207–1220.

39. Hashimoto, Y., Zhang, S., Zhang, S., Chen, Y.R., and Blissard, G.W. (2012). Correction: BTI-Tnao38, a new cell line derived from Trichoplusia ni, is permissive for AcMNPV infection and produces high levels of recombinant proteins. BMC Biotechnol. *12*, 12.

40. Bonnet, C., Lassueur, S., Ponzio, C., Gols, R., Dicke, M., and Reymond, P. (2017). Combined biotic stresses trigger similar transcriptomic responses but contrasting resistance against a chewing herbivore in *Brassica nigra*. BMC Plant Biol. *17*, 127.

41. Schneider, C.A., Rasband, W.S., and Eliceiri, K.W. (2012). NIH Image to ImageJ: 25 years of image analysis. Nat. Methods *9*, 671–675.

42. Cox, J., and Mann, M. (2008). MaxQuant enables high peptide identificationrates, individualized p.p.b.-range mass accuracies and proteome-wide protein quantification. Nat. Biotechnol. *26*, 1367–1372.

43. Tyanova, S., Temu, T., Sinitcyn, P., Carlson, A., Hein, M.Y., Geiger, T., Mann, M., and Cox, J. (2016). The Perseus computational platform for comprehensive analysis of (prote)omics data. Nat. Methods *13*, 731–740.

44. Perez-Riverol, Y., Bai, J., Bandla, C., García-Seisdedos, D., Hewapathirana, S., Kamatchinathan, S., Kundu, D.J., Prakash, A., Frericks-Zipper, A., Eisenacher, M., et al. (2022). The PRIDE database resources in 2022: a hub for mass spectrometry-based proteomics evidences. Nucleic Acids Res. *50*, D543–D552.

45. Kulak, N.A., Pichler, G., Paron, I., Nagaraj, N., and Mann, M. (2014). Minimal, encapsulated proteomic-sample processing applied to copy-number estimation in eukaryotic cells. Nat. Methods *11*, 319–324.

46. Cox, J., Neuhauser, N., Michalski, A., Scheltema, R.A., Olsen, J.V., and Mann, M. (2011). Andromeda: a peptide search engine integrated into the MaxQuant environment. J. Proteome Res. *10*, 1794–1805.

47. Schwanhäusser, B., Busse, D., Li, N., Dittmar, G., Schuchhardt, J., Wolf, J., Chen, W., and Selbach, M. (2011). Global quantification of mammalian gene expression control. Nature *473*, 337–342.

48. Li, X., and Kushad, M.M. (2005). Purification and characterization of myrosinase from horseradish (*Armoracia rusticana*) roots. Plant Physiol. Biochem. *43*, 503–511.

49. Oñate-Sánchez, L., and Vicente-Carbajosa, J. (2008). DNA-free RNA isolation protocols for *Arabidopsis thaliana*, including seeds and siliques. BMC Res. Notes *1*, 93.

50. Gfeller, A., Baerenfaller, K., Loscos, J., Chételat, A., Baginsky, S., and Farmer, E.E. (2011). Jasmonate controls polypeptide patterning in undamaged tissue in wounded *Arabidopsis* leaves. Plant Physiol. *156*, 1797–1807.

51. Farmer, E.E., and Kurenda, A. (2018). Rapid extraction of living primary veins from the leaves of *Arabidopsis thaliana*. Protoc. Exch. https://doi.org/10.1038/protex.2018.119.

52. Glauser, G., Schweizer, F., Turlings, T.C., and Reymond, P. (2012). Rapid profiling of intact glucosinolates in *Arabidopsis* leaves by UHPLC-QTOFMS using a charged surface hybrid column. Phytochem. Anal. *23*, 520–528.

STAR★METHODS

KEY RESOURCES TABLE

REAGENT or RESOURCE	SOURCE	IDENTIFIER
Antibodies		
Anti-His_6-Peroxidase	Sigma-Aldrich	Cat#11965085001, RRID:AB_514487
Bacterial and virus strains		
DH10 MultiBac *E.coli* Cells	Geneva Biotech	https://geneva-biotech.com/product_category/insect-cell-expression/multibac/
Chemicals, peptides, and recombinant proteins		
Acetonitrile	Sigma-Aldrich	Cat#34851
Ammonia	Sigma-Aldrich	Cat#294993
Basic fuchsin	Sigma-Aldrich	Cat#857343
Bromophenol blue sodium salt	Sigma-Aldrich	Cat#B8026
Chloroacetamide	Sigma-Aldrich	Cat#22790
dATPs; dGTPs; dCTPs; dTTPs;	Promega	Cat#U1205; Cat#U1215; Cat#U1225; Cat#U1235
d-Desthiobiotin	Sigma-Aldrich	Cat#D1411
Dithiothreitol	Sigma-Aldrich	Cat#D9163
EDTA	Sigma-Aldrich	Cat#03609
Ethanol	Sigma-Aldrich	Cat#51976
Fluorescein isothiocyanate–dextran (FITC-dextrans): average mol wt 3,000-5,000; 40,000; 500,000	Sigma-Aldrich	Cat#FD4; Cat#FD40S; Cat#FD500S
Formaldehyde	Sigma-Aldrich	Cat#47608
Formic acid	Sigma-Aldrich	Cat#33015
Glutaraldehyde	Sigma-Aldrich	Cat#G5882
Glucoraphanin potassium salt	Sigma-Aldrich	Cat#PHL89215
Glucohesperin potassium salt	Sigma-Aldrich	Cat#PHL85746
Glucobrassicin potassium salt	Sigma-Aldrich	Cat#PHL80593
Glycerol	Sigma-Aldrich	Cat#G5516
GoTaq DNA polymerase	Promega	Cat#M3005
HEPES	Sigma-Aldrich	Cat#H3375
Hydrochloric acid	Sigma-Aldrich	Cat#320331
Imidazole	Sigma-Aldrich	Cat#I5513
L-Ascorbic acid	Sigma-Aldrich	Cat#A92902
L-Glutamic acid	Sigma-Aldrich	Cat#49449
Methanol	Sigma-Aldrich	Cat#34860
Paraffin oil	Fluka	Cat#76235
Pierce™ 1-step transfer buffer	Thermo Fisher Scientific	Cat#84731
Potassium chloride	Sigma-Aldrich	Cat#P9541
Potassium phosphate dibasic	Sigma-Aldrich	Cat#795496
Potassium phosphate monobasic	Sigma-Aldrich	Cat#P0662
Recombinant TGG1 protein	This paper	N/A
Recombinant TGG1-E420N protein	This paper	N/A
Recombinant TGG1-E420A protein	This paper	N/A
Recombinant TGG1-StrepII-9×His protein	This paper	N/A
ROX reference dye	Thermo Fisher Scientific	Cat#12223012
(−)-Sinigrin hydrate (sinigrin)	Sigma-Aldrich	Cat#85440
Sodium chloride	Sigma-Aldrich	Cat#S5886

(*Continued on next page*)

Continued

REAGENT or RESOURCE	SOURCE	IDENTIFIER
Sodium deoxycholate	Sigma-Aldrich	Cat#D6750
Sodium dodecyl sulfate	Sigma-Aldrich	Cat#L3771
Sodium phosphate	Sigma-Aldrich	Cat#342483
Sodium fluorescein	Sigma-Aldrich	Cat#F6377
SYBR Green I	Thermo Fisher Scientific	Cat#S7563
Magnesium chloride	Sigma-Aldrich	Cat#M8266
MES (4-Morpholineethanesulfonic acid)	Sigma-Aldrich	Cat#M3671
M-MLV reverse transcriptase, RNase H Minus, Point Mutant	Promega	Cat#M3682
MOPS	Sigma-Aldrich	Cat#69947
TEV protease	New England Biolabs	Cat#P8112S
Toluidine blue	Sigma-Aldrich	Cat#89640
Tris base	Sigma-Aldrich	Cat#T1503
Trifluoroacetic acid (TFA)	Sigma-Aldrich	Cat#302031
Trypsin/LysC mix	Promega	Cat#V5073
Tween 20	Sigma-Aldrich	Cat#P1379
Western blocking reagent	Sigma-Aldrich	Cat#11921681001
Western bright sirius HRP substrate	Advansta	Cat#K-12043-C20
Critical commercial assays		
Gel Filtration Calibration Kit LMW and HMW	Cytiva	Cat#28403841; Cat#28403842
Deposited data		
Raw peptide data	This paper, see www.proteomexchange.org	PXD031220
Experimental models: Cell lines		
Spodoptera frugiperda Sf9	Thermo Fisher Scientific	Cat#B82501
Trichoplusia ni Tnao38 cells	Hashimoto et al.[39]	N/A
Experimental models: Organisms/strains		
Arabidopsis: Col-0	NASC	NCBI Taxonomy ID:3702
glr3.3	Mousavi et al.[6]	SALK_099757
glr3.6	Mousavi et al.[6]	SALK_ 091801
GCaMP3 WT (*UBQ10pro::GCaMP3* in Col-0)	Nguyen et al.[9]	N/A
GCaMP3 *glr3.3*	Nguyen et al.[9]	N/A
GCaMP3 *glr3.6*	Nguyen et al.[9]	N/A
GCaMP3 *glr3.3 glr3.6*	Nguyen et al.[9]	N/A
GCaMP3 *tgg1tgg2*-29/43	This paper	N/A
myb28 myb29	Sønderby et al.[23]	N/A
tgg1	NASC	SAIL_786_B08
tgg1a	NASC	SALK_093296
tgg2	NASC	SALK_038730
tgg2a	NASC	SALK_035702
tgg3	NASC	SALK_206359
tgg3a	NASC	SALK_085567
tgg1 tgg2	Barth and Jander[21]	NASC ID: N72545
tgg1 tgg3	This paper	N/A
tgg2a tgg3	This paper	N/A
tgg1 tgg2 tgg3	This paper	N/A
tgg1 tgg2 glr3.3	This paper	N/A

(*Continued on next page*)

Continued

REAGENT or RESOURCE	SOURCE	IDENTIFIER
tgg1 tgg2 glr3.6	This paper	N/A
Pieris brassicae larvae	Bonnet et al.[40]	N/A
Aphid (*Brevicoryne brassicae* L.)	Grown in house	N/A
Oligonucleotides		
*JAZ10*_forward: 5'-ATCCCGATTTCTCCGGTCCA-3'	This paper	N/A
*JAZ10*_reverse 5'-ACTTTCTCCTTGCGATGGGAAGA-3'	This paper	N/A
*UBC21*_forward: 5'-CAGTCTGTGTGTAGAGCTAT CATAGCAT-3'	This paper	N/A
*UBC21*_reverse: 5'-AGAAGATTCCCTGAGTCGCAGTT-3'	This paper	N/A
TGG1-E420N_forward: 5'-CTACGTCACCAACAACGGT TTCTCTACCCCTG-3'	This paper	N/A
TGG1-E420N_reverse: 5'-GAAACCGTTGTTGGTGACG TAGATCAGAGG-3'	This paper	N/A
TGG1-E420A_ forward: 5'-CTACGTCACCGCGAACGG TTTCTCTACCCCTG-3'	This paper	N/A
TGG1-E420A_ reverse: 5'-GAAACCGTTCGCGGTGAC GTAGATCAGAGG-3'	This paper	N/A
T-DNA genotyping primers, see Table S2	This paper	N/A
Recombinant DNA		
TGG1-Glu420Asn-StrepII-9×His	This paper	N/A
TGG1-Glu420Ala-StrepII-9×His	This paper	N/A
TGG1-StrepII-9×His	This paper	N/A
Software and algorithms		
ChemDraw v20.0	PerkinElmer	RRID:SCR_016768
Fiji (ImageJ)	Schneider et al.[41]	RRID:SCR_002285
GraphPad Prism 8.0.2 (263)	GraphPad Software Inc.	RRID:SCR_002798
LabScribe4 software	iWorx Systems, Inc.	https://iworx.com/labscribe-software-download/
MaxQuant software (version 1.6.3.4)	Cox and Mann[42]	RRID:SCR_014485
Masslynx 4.2	Waters	RRID:SCR_014271
NIS-Elements imaging software	Nikon	RRID:SCR_014329
Perseus software	Tyanova et al.[43]	RRID:SCR_015753
SigmaPlot 14.0	Systat Software Inc	RRID:SCR_003210
Stylet$^+$ software	EPG systems	www.epgsystems.eu
TargetLynx software	Waters	https://www.waters.com/waters/en_US/TargetLynx-/nav.htm?cid=513791&locale=en_US
Xcalibur 4.2 software	Thermo Fisher Scientific	RRID:SCR_014593
Other		
DEAE Sepharose Fast Flow resin	Sigma-Aldrich	Cat#GE17-0709-01
HiLoad 16/600 Superdex 200 pg column	Cytiva	Cat#28989335
HisTrap excel column	Cytiva	Cat#17371205
Manual micromanipulator	World Precision Instruments	Cat#M3301R
Nitrocellulose blotting membranes (Amersham Protran 0.45 μm)	Cytiva	Cat#10600062
Oasis MCX 96-well Plate	Waters	Cat#186000248
Pierce™ Protein Concentrator PES, 3K MWCO, 5-20 mL	Thermo Fisher Scientific	Cat#88525
Strep-Tactin Superflow high capacity column	IBA Lifesciences	Cat#2-1209-051
Superdex 75 Increase HiScale 16/40 size-exclusion column	Sigma-Aldrich	Cat#GE29321907

(*Continued on next page*)

Continued

REAGENT or RESOURCE	SOURCE	IDENTIFIER
Superdex 200 10/300 GL column	Cytiva	Cat#17517501
Technovit 7100 resin	Haslab	Cat#8910005
Tungsten carbide beads	Qiagen	Cat#69997
XK 26/40 column	Cytiva	Cat#28988949

RESOURCE AVAILABILITY

Lead contact

Further information and requests for plant materials may be directed to and will be fulfilled by the lead contact, Edward E. Farmer (edward.farmer@unil.ch).

Materials availability

Plant seeds generated in this study will be made available on request.

Data and code availability

- The mass spectrometry proteomics data have been deposited to the ProteomeXchange Consortium (www.proteomexchange.org) via the PRIDE partner repository.[44]
- This study did not generate any code.
- Any additional information required to reanalyze the data reported in this paper is available from the lead contact upon request.

EXPERIMENTAL MODEL AND SUBJECT DETAILS

Plant materials

Wild-type (WT) and mutant *Arabidopsis thaliana* were all in the Columbia (Col) genetic background and were obtained from Nottingham *Arabidopsis* Stock Centre: *tgg1* (AT5G26000) SAIL_786_B08; *tgg1a* (AT5G26000) SALK_093296; *tgg2* (AT5G25980) SALK_038730; *tgg2a* (AT5G25980) SALK_035702; *tgg3* (AT5G48375) SALK_206359; *tgg3a* (AT5G48375) SALK_085567. The *tgg1 tgg2* double mutant described in Barth and Jander[21] was supplied by G. Jander (Cornell, USA). The *myb28 myb29* mutant was from Sønderby et al.[23] The *gtr1 gtr2* mutant was from Nour-Eldin et al.[24] The following cross was performed to select the *tgg1 tgg2 tgg3* triple mutant: SALK_206359 (♂) × *tgg1 tgg2* (♀). The following cross was performed to select the *tgg1 tgg3* double mutant: SAIL_786_B08 (♂) × SALK_206359 (♀), and the *tgg2a tgg3* double mutant: SALK_206359 (♂) × SALK_035702 (♀).The *glr3.3* (SALK_099757), *glr3.6* (SALK_ 091801), and *glr3.3 glr3.6* (SALK_099757, SALK_ 091801) mutants were from Mousavi et al.[6] Crosses of *glr3.3* (♂) × *tgg1 tgg2* (♀), *glr3.6* (♂) × *tgg1 tgg2* (♀) were performed to select triple mutants. Primers used for T-DNA mutant genotyping are given in Table S2. WT, *glr3.3*, *glr3.6,* and *glr3.3 glr3.6* plants expressing GCaMP3 were from Nguyen et al.[9] 5-6 week-old plants were used for all experiments.

Plant growth conditions

Seeds were planted on soil (Professional Horticulture Substrate, Jiffy Products International, Zwijndrecht, Netherlands) in 7 cm diameter pots and stratified at 4°C for 2 days then moved into the following growth conditions: 10 h light (100-120 μE m^{-2} s^{-1}) at 22°C and 14 h dark at 18°C. Relative humidity was maintained at 70%. These conditions were maintained for all experiments including those in Faraday cages.

METHOD DETAILS

Non-invasive electrophysiology

Surface electrophysiology including quantification of SWP amplitudes and durations was described in Mousavi et al.[6] Two 2-channel amplifiers (FD 223 and Duo 773, World Precision Instruments, Friedberg, Germany) were used to record the surface potential in a Faraday cage. Silver electrodes (0.5 mm diameter) were chloridized with 0.1 M HCl, and re-chloridized whenever necessary until most of the baseline fluctuations were eliminated. Plants were connected to silver electrodes with drops of conducting solution (5 μL of 10 mM KCl in 50% [v/v] glycerol). A reference electrode was placed in the soil. Electrical signals were acquired at 100 Hz and analysed using LabScribe4 software (iWorx Systems, Inc., Dover, NH, USA). Aluminum foil was used to wrap the leaf lamina for shading. Paraffin oil was applied by dipping the leaf lamina in the oil. Plants were used 3 h after treatment. Each experiment was repeated at least twice with similar results. Analyses of amplitudes and durations is shown in Figure 1A, where amplitude is the difference of voltage between baseline and maximum depolarization (amplitude = $Voltage_{max\text{-}depolarization}$ − $Voltage_{baseline}$).

Duration is from the time the electrical signals reaches half-maximum depolarization voltage to that when they re-reach the half-maximum depolarization voltage during the repolarization phase (duration = $t_{1/2\ repolarization} - t_{1/2\ depolarization}$). Velocities of SWPs were calculated using the following formula: $V_{SWP} = 1/\Delta t_{E2\text{-}E1}$, E1 and E2 were 1 cm apart, $\Delta t_{E2\text{-}E1}$ is the time difference when SWP reaches half-maximum depolarization voltage in E2 and E1.

Electrical Penetration Graphs

Phloem sieve element wound signals were recorded by Electrical Penetration Graphs (EPGs), which were performed in a Faraday cage. 5-6 week-old *Arabidopsis* plants were used in the experiments. Preparation of aphid electrodes, recording processes and quantification of signal duration and amplitude were as described[19] except that an eight channel direct current system was used for recording (Giga-8dd, Basic EPG Systems, Wageningen, Netherlands). *Stylet*$^{+}$ software (EPG systems) was used for data acquisition and analysis. Aphids (*Brevicoryne brassicae* L.) were restricted to feed on the midrib in the middle of the leaf 13 lamina. 50% of leaf 8 on the same plant was crush-wounded with forceps to induce wound electrical signals.

Stepwise cutting of petioles

The petioles of leaf 8 were stabilized by placing wooden tooth picks in the soil to avoid petiole movement during transverse step cuts. A vertically fixed scalpel blade on a manual micromanipulator (M3301, World Precision Instruments, Hitchin, UK) was used for successive 100 μm cuts. The blade was moved to touch the margin of petiole 8 before the first cut. Surface potential recording and step cuts were performed simultaneously. Each successive cut was made when baseline electrical potential changes following cutting had been re-established (i.e. when membranes had repolarized). This experiment was successfully repeated twice with different batches of plants.

Fuchsin staining, fluorescein-sodium/fluorescein isothiocyanate–dextran application and data analyses

Leaf 8 petioles of 5-6 week-old plants were cut in 0.01% (w/v) basic fuchsin (Sigma-Aldrich, Buchs, Switzerland) solution (1 mL) and kept in the staining solution for 4 h. Hand-cut transverse petiole and hypocotyl sections were imaged with Leica DM5500 microscope. Under illumination with white light (bright field), basic fuchsin was seen to have spread from the severed leaf 8 petiole into much of the nearby vasculature. With 560 ± 80 nm excitation and 645 ± 150 nm detection, autofluorescence from the xylem vessel was avoided by using low intensity excitation light. Xylem vessel autofluorescence and fluorescence from some of the stained vasculature cells were not visible because of their low intensity compared to the strong lignin staining of xylem vessels.

Sodium fluorescein (NaFluo) and fluorescein isothiocyanate-dextrans (FITC-dextrans, Sigma-Aldrich, Buchs, Switzerland) were applied at 1 mg mL^{-1} in Milli-Q (Merck, Darmstadt, Germany) water to the intact leaf petiole of 5-6 week-old WT plants. A piece of cardboard was inserted between leaf 8 and leaf 13 to block fluorescence from the fluorescein solution in which petiole 8 was immersed. Systemic propagation of fluorescence in distal leaf 13 after cutting the intact petiole with scissors was recorded on an ORCA-Flash4.0 (C11440) camera (Hamamatsu, Solothurn, Switzerland) with eGFP emission/excitation filter set (AHF analysentechnik AG, Tübingen, Germany) on an SMZ18 stereomicroscope (Nikon Instruments Europe BV, Amsterdam, Netherlands). Videos (1 frame s^{-1}) with resolution of 512×512 pixels in each frame were acquired using NIS-Elements software (Nikon). Intensity of fluorescence from regions of interest (ROIs = 50 pixels) on the petiole 13 were analysed using Fiji/image J (http://fiji.sc/Fiji). Background signal was subtracted from the fluorescence. Travel velocities of NaFluo and FITC-dextrans were calculated using the following formula: $V_{Fluo.} = 1/\Delta t_{ROI2\text{-}ROI1}$, ROI1 and ROI2 were 1 cm apart, $\Delta t_{ROI2\text{-}ROI1}$ is the time difference when fluorescence reaches half-maximum intensity in ROI2 and ROI1. Leaves were shaded by carefully wrapping the lamina with aluminum foil and plants were used 3 h after shading. In most cases, chemicals were fed into the severed leaf 8 petiole and fluorescence was analysed in leaf 13. In the case of feeding chemicals from leaf 13, fluorescence in leaf 8 was analyzed. These chemical tracing assays were repeated at least twice with similar results.

Microscopy for petiole transversal sections

Three hours after scalding, petioles were fixed in glutaraldehyde / formaldehyde / 50 mM sodium phosphate (pH 7.2) 2:5:43 (v/v/v) overnight at 4 °C. The samples were dehydrated in an ethanol step gradient (10%, 30%, 50%, 70%, 90% and twice absolute ethanol, 30 min in each concentration), and embedded in Technovit 7100 resin (Haslab GmbH, Ostermundigen, Switzerland) according to the manufacturer's instructions. Transversal petiole sections (5 μm thick) were cut on a RM2255 microtome (Leica, Wetzlar, Germany). The sections were stained with 0.1% (w/v) toluidine blue (Sigma-Aldrich, Buchs, Switzerland) in water for 3 minutes. Then briefly rinsed with water, air-dried at room-temperature and photographed with a Leica Thunder DM5400 microscope.

Crush wounding

Forceps with ridges placed in parallel to the long axis of the leaf were used for crush wounding. 50% of the leaf 8 apical region was crush wounded using a single wound (taking approximately 2 s) to initiate responses in distal leaf 13.

Petiole scalding and Ricca's factor assay development

Around 5 mm petiole was scalded by rapidly pipetting 100-200 μL boiling water onto the petiole midway between the petiole base and the lamina. Excess water on the petiole was removed with tissue paper. This process takes approximately 30 s per plant. One leaf

petiole was scalded per plant and experiments were performed 3-6 hours after scalding. For treatments with leaf extracts, recombinant proteins or small molecules, solutions of 60-70 μL in a container (lid of 0.5 mL Eppendorf tube, inner diameter 5 mm, depth 2 mm; Kartell Labware, Noviglio, Italy) were placed under the scalded petiole. We ensured that the scalded petiole was immersed in the solution, then the scalded section was cut with a surgical scissors. Throughout the procedure plants were maintained in the light at 22°C. Individual plants were not used more than once.

Leaf extract preparation

The expanded rosette leaves from 5-6 week-old *Arabidopsis* plants were collected and ground to powder in liquid nitrogen with a mortar. This powder was either stored at -80°C for future use or centrifuged at 12,000 g at 10°C for 10 min for immediate use. The supernatant after centrifugation was collected and is referred to as fresh leaf extract (FLE).

Ricca's factor purification: anion-exchange chromatography and size-exclusion chromatography

Fresh leaf extract (10 mL) from 5-6 week-old WT *A. thaliana* leaves was diluted with 90 mL 50 mM Tris-HCl, pH 8.0. The diluted sample was loaded onto an XK 26/40 column (Cytiva, Glattbrugg, Switzerland) packed with 100 mL of DEAESepharose Fast Flow resin (Cytiva, Glattbrugg, Switzerland) that had been equilibrated with 200 mL 50 mM Tris-HCl, pH 8.0. After loading the sample, resin was washed with 200 mL 50 mM Tris-HCl, pH 8.0 to remove unbound solutes. A linear gradient of NaCl from 0 mM to 500 mM was applied to elute bound molecules at a flow rate of 2 mL min^{-1}, and 13 mL fractions were collected. The collected fractions were diluted 2-fold with 50 mM Tris-HCl, pH 8.0 for biological activity tests using the Ricca's factor assay.

Highly active fractions (fractions 57-61) were combined, concentrated and buffer-exchanged into size-exclusion chromatography elution buffer: 50 mM Tris-HCl, pH 8.0 containing NaCl (200 mM) using 3 K molecular weight cut-off ultrafiltration concentrators (Pierce, Thermo Fisher Scientific, Reinach, Switzerland). Further fractionation was performed on a Superdex 75 Increase HiScale 16/40 size-exclusion column (Cytiva, Glattbrugg, Switzerland). The column was first washed with two bed volumes of Milli-Q water then equilibrated with two bed volumes of elution buffer. All fractionation processes were performed at 4-10°C. After loading the sample, 1.5 bed volumes of elution buffer were used with a flow rate of 0.8 mL min^{-1}. Fractions (3 mL) were collected and were further diluted 2-fold with 50 mM Tris-HCl, pH 8.0 for biological activity tests and for peptide analyses.

Protein digestion for LC-MS/MS

Fractions from size-exclusion chromatography were digested using the miST method.[45] Each protein fraction (20 μL) was mixed with 25 μL miST lysis buffer consisting of sodium deoxycholate (1% w/v) and dithiothreitol (10 mM) in 100 mM Tris pH 8.6. Samples were then heated at 95°C for 5 min and then diluted 1:1 (v:v) with water. Reduced disulfides were alkylated by adding 11 μL of 160 mM chloroacetamide and incubating at 25°C for 45 min in the dark. Samples were adjusted to 3 mM EDTA and digested with 0.5 μg Trypsin/LysC mix (Promega, Dübendorf, Switzerland) for 1 h at 37°C. This was followed by a second 1 hour digestion with a second and identical aliquot of proteases. For elimination of deoxycholate, two sample volumes of isopropanol containing 1% (v/v) trifluoroacetic acid (TFA) were added to the digests. Each sample was then desalted using an Oasis MCX plate (Waters Corp., Milford, MA) by centrifugation. After washing with isopropanol containing 1% (v/v) TFA, peptides were eluted in 250 μL of 80% acetonitrile, 19% water, and 1% (v/v) ammonia.

Liquid chromatography-tandem mass spectrometry for peptides

Desalted eluates were dried and resuspended in 50 μL trifluoroacetic acid (0.05% v/v), 2% acetonitrile (2% v/v) in water. Samples (4 μL) were injected on-column for nanoLC-MS analysis. Data-dependent LC-MS/MS peptide analyses were carried out on a Fusion Tribrid Orbitrap mass spectrometer (Thermo Fisher Scientific, Reinach, Switzerland) interfaced through a nano-electrospray ion source to an Ultimate 3000 RSLCnano HPLC system (Dionex, Reinach, Switzerland). Peptides were separated on a custom-packed reversed-phase 40 cm C18 column (75 μm internal diametre, 100Å, Reprosil Pur 1.9 μm particles, Dr. Maisch, Ammerbuch-Entringen, Germany) with a 4-76% acetonitrile gradient in 0.1% formic acid (total run time 45 min). Full MS survey scans were performed at 120,000 resolution. A data-dependent acquisition method controlled by Xcalibur 4.2 software (Thermo Fisher Scientific) was used to optimize the number of precursors selected of charge 2^+ to 5^+ while maintaining a fixed scan cycle of 1.5 s. The precursor isolation window used was 0.7 Th. Full survey scans were performed at a 120,000 resolution, and a top speed precursor selection strategy was applied to maximize acquisition of peptide tandem MS spectra with a maximum cycle time of 0.6 s. HCD fragmentation mode was used at a normalized collision energy of 32%, with a precursor isolation window of 1.6 *m/z*, and MS/MS spectra were acquired in the ion trap. Peptides selected for MS/MS were excluded from further fragmentation during 60 s.

MS peptide analyses

Tandem MS data were processed with MaxQuant software version 1.6.3.4[42] incorporating the Andromeda search engine.[46] The *A. thaliana* reference proteome (RefProts) database of November 2019 was used (39,362 sequences), supplemented with sequences of common contaminants. Trypsin (cleavage at K, R) was used as the enzyme definition, allowing 2 missed cleavages. Carbamidomethylation of cysteine was specified as a fixed modification. N-terminal acetylation of protein and oxidation of methionine were

specified as variable modifications. All identifications were filtered at 1% FDR at both the peptide and protein levels with default MaxQuant parameters. MaxQuant data were further processed with Perseus software.[43] iBAQ[47] values were used for quantitation after $\log_2$ transformation.

Protein expression and purification from insect cells

Synthetic TGG1 codon-optimized for *Spodoptera frugiperda* (At5g26000; residues 20 to 541) was synthesized by Invitrogen GeneArt (Thermo Fisher Scientific, Reinach, Switzerland). The gene was cloned into a modified pFastBac donor vector (Geneva Biotech, Geneva, Switzerland) harboring the *Drosophila BiP* secretion signal peptide, and with a TEV (tobacco etch virus) protease-cleavable C-terminal StrepII-9×His tag. TGG1-donor vector construct was transformed into DH10 MultiBac *E.coli* Cells (Geneva Biotech) to produce a recombinant TGG1 bacmid. TGG1 baculovirus was produced in *Spodoptera frugiperda* Sf9 cells (Thermo Fisher Scientific, Reinach, Switzerland) from the TGG1 bacmid. For protein expression, *Trichoplusia ni* Tnao38 cells[39] were infected with TGG1 baculovirus with a multiplicity of infection (MOI) of 3 and incubated with continuous shaking (110 rpm) at 28 °C for 1 d and 22 °C for 2 d. The secreted TGG1 protein was purified from the supernatant by Ni^{2+} affinity chromatography (HisTrap excel column; Cytiva, Glattbrugg, Switzerland) equilibrated in 25 mM potassium phosphate buffer, pH 7.8 containing 500 mM NaCl. Recombinant TGG1 proteins were eluted with 25 mM potassium phosphate buffer, pH 7.8 containing 500 mM NaCl and 500 mM imidazole.

The eluate was subjected to StrepII affinity chromatography using a Strep-Tactin Superflow high capacity column (IBA Lifesciences, Göttingen, Germany) equilibrated in 25 mM Tris, pH 8.0 buffer containing 1 mM EDTA, 250 mM NaCl and eluted with 25 mM Tris, pH 8.0 containing 1 mM EDTA, 250 mM NaCl, 3.5 mM d-desthiobiotin. Proteins were then incubated with TEV protease (50:1 ratio, TGG1:TEV) overnight at 4°C to cleave the tags. The TEV protease and cleaved tags were removed by Ni^{2+} affinity chromatography. Proteins were further purified by size-exclusion chromatography on a HiLoad 16/600 Superdex 200 pg column (Cytiva, Glattbrugg, Switzerland) equilibrated with 20 mM HEPES buffer, pH 7.5, containing 150 mM NaCl. Calculation of molar quantities of recombinant TGG1 were based on a predicted mass of 60.4 kDa (from the coding sequence plus 10 additional C-terminal amino acids left after cleavage of the StrepII and His purification tags. Catalytically inactive versions of TGG1: TGG1-Glu420Asn and TGG1-Glu420Ala were generated through site directed mutagenesis using the codon optimized constructs (GeneArt, Thermo Fisher Scientific, Reinach, Switzerland) for insect cell expression of TGG1 with the following primers: TGG1-E420N_forward/reverse and TGG1-E420A_forward/reverse, see key resources table.

Analytical size-exclusion chromatography

Purified TGG1 (500 μL at 5 μM) was injected into a Superdex 200 10/300 GL column (Cytiva, Glattbrugg, Switzerland) pre-equilibrated in 20 mM HEPES pH 7.5 buffer containing 150 mM NaCl. The estimation of apparent molecular size was done following the calibration curve obtained using proteins standards from gel filtration calibration kits LMW and HMW: aprotinin (6.5 kDa), ribonuclease A (13.7 kDa), carbonic anhydrase (29.0 kDa), ovalbumin (44.0 kDa), conalbumin (75.0 kDa), aldolase (158.0 kDa), ferritin (440.0 kDa) and blue dextran 2000 (Cytiva, Glattbrugg, Switzerland).

Myrosinase activity assays

Myrosinase activity was determined using sinigrin as a substrate.[21,48] Sinigrin hydrolysis was monitored at 227 nm using a UV spectrophotometer (GENESYS 10S UV-VIS, Thermo Fischer Scientific, Lindau, Switzerland). The reaction mixture contained 0.2 mM Sinigrin (Sigma-Aldrich, Buchs, Switzerland), 0.3 mM L-ascorbic acid (Fluka, Buchs, Switzerland) in 50 mM MES, pH 6.0 with Tris. 1 μL recombinant TGG1 protein (3.6 μg μL^{-1}) was added to the mixture to initiate the reaction. Decline in absorbance at 227 nm was monitored for 5 min at 30 s intervals at room temperature (24°C). The linear phase of absorbance decline was used to calculate the enzyme activity (0 to 5 min). Myrosinase activity was calculated according to the following formulae: ΔC (mol/L) = $\Delta A/\varepsilon l$, Δn (mmol) = $\Delta C V_T$, myrosinase activity (μmol sinigrin min^{-1} μg^{-1} protein) = $10^3 \Delta n V_T / t m V_S$, where ΔC is the total amount of hydrolyzed sinigrin in 5 min, ΔA is the absorbance change, ε is the molar extinction coefficient of sinigrin derived from a sinigrin standard (ε = 7275 M^{-1} cm^{-1}), l is the cuvette path length (1 cm), V_T is the total volume of reaction mixture (1 mL), Δn is total amount of hydrolyzed sinigrin in 5 min in 1 mL reaction mixture, t is the time of reaction (5 min), m is the amount of protein (3.6 μg), V_s is the total volume of protein sample (1 μL) used for each reaction. Myrosinase activity of fresh leaf extract was calculated by using the volume of extracts applied (5 μL) instead of the amount of protein. At least 4 independent replicates were used for each assay. Each assay was successfully repeated at least twice.

Pieris brassicae larvae feeding assays

Assays were performed according to Kurenda et al.[14] *Pieris brassicae* larvae raised on cabbage[40] were transferred to 5–6 weeks old *Arabidopsis* for at least 24 h before experiment, then 4th or 5th instar *Pieris brassicae* larvae were starved for 2 h. The petiole of leaf 8 was passed through a 3 mm vertical slit in the side wall of a plastic Petri dish (5.5 cm in diameter) and covered with a plastic lid after placing larvae on leaf 8. For simultaneous larval feeding and surface potential recording, feeding was stopped after the slow wave potential reached distal leaf 13, or after the lamina of leaf 8 was completely consumed without the initiation of surface potential changes (eg. for many recordings from *tgg1 tgg2* plants). The insect feeding assays were successfully repeated at least three times independently. For gene expression analyses, 3 larvae per Petri dish were used to accelerate the feeding process. Larval feeding was stopped when the leaf 8 lamina was cut off from the petiole, or the lamina of leaf 8 was completely consumed (typically taking 5-15 min). For gene expression analyses leaf 13 was sampled 1 h after larval feeding.

Gene expression analyses

DNA free leaf total RNA was extracted from leaf samples.[49] 1 μg total RNA was copied into complementary DNA with the M-MLV reverse transcriptase, RNase H Minus, Point Mutant (Promega, Dübendorf, Switzerland) according to the manufacturer's instructions. Quantitative PCR was performed with an Applied Biosystems QuantStudio 3 Real-Time PCR System (Thermo Fisher Scientific, Reinach, Switzerland) used methods described by Gfeller et al.[50] The mixture contained 0.2 mM dNTPs, 2.5 mM $MgCl_2$, 0.5×SYBR Green I (Invitrogen, Thermo Fisher Scientific), 30 nM ROX reference dye (Thermo Fisher Scientific), 0.5 units GoTaq DNA polymerase (Promega, Dübendorf, Switzerland), and 0.25 mM of each primer (Microsynth AG, Balgach, Switzerland), in a final volume of 20 μL. The PCR program consisted of a 2 min initial denaturation step at 95°C, followed by 40 cycles of 10 s at 95°C, 30 s at 60°C, and 30 s at 72°C. Real-timePCR data were analysed using the $2^{-\Delta\Delta CT}$ method. Primers for reference gene *UBC21* (*Ubiquitin-conjugating enzyme 21*; AT5G25760) and *JAZ10* (*JASMONATE ZIM-DOMAIN 10*; AT5G13220) are included in the KEY RESOURCES TABLE. At least four replicates were used for each qPCR experiment. Experiments were repeated at least twice with similar results.

Calcium imaging and data analysis

Cytosolic Ca^{2+} transients were visualized with 5-6 week-old WT plants and *glr* mutants expressing GCaMP3[9] and in *tgg1 tgg2* plants in which the GCaMP3 transgene was introgressed from the same WT background. Two independent GCaMP3 *tgg1 tgg2* homozygous F3 lines were used. GCaMP3 florescence was captured by using the same setup and setting for fluorescein as described above. Fluorescence from the whole distal leaf 13, including the petiole, was analyzed using Fiji/image J (http://fiji.sc/Fiji). Transient cytosolic Ca^{2+} changes are indicated as $\Delta F/F = (Fx\text{-}F)/F$. *Fx* is the fluorescent intensity from the moment of crush wounding or cutting the scalded petiole region to a given time-point, *F* is the baseline fluorescence intensity in the ROIs calculated from the first 10 s fluorescence after wounding.

Glucosinolate analyses with extracted veins

Approximately 60% of the apical lamina surface of a single expanded leaf of a 5.5 week-old plant was wounded. Two min after the completion of wounding, a primary vein was extracted from a juxtapositioned distal leaf according to protocol number 2 in Farmer and Kurenda.[51] Vein samples (10-15 mg, from an average of 15 plants) were placed in chilled 2 mL Safe-Lock Eppendorf tubes (Eppendorf, Hamburg, Germany). After weighing, 2 pre-chilled tungsten carbide beads (3 mm diameter, Qiagen, Hilden, Germany) were added and the samples were stored prior to extraction. Frozen samples were ground for 10 s in the Qiagen TissueLyser II (Qiagen, Hilden, Germany) at 30 Hz. Then, water/methanol/formic acid (30:70:0.1, v/v; 0.2 mL) was added. Tubes were vortexed for 10 s then shaken twice for 1.25 min at 30 Hz. In between each round of shaking tube lids were re-tightened and tubes were then briefly inverted. The tubes were then centrifuged at 10,000 g for 2.5 min. Supernatant (>100 μL) that was free of particles was transferred to an HPLC vial containing a 250 μL conical insert.

Glucosinolate analyses were performed on an Acquity UPLC I-Class coupled to a Synapt XS Q-TOF mass spectrometer (Waters, Milford, MA, USA) using a method adapted from Glauser et al.[52] The column used for separation was an Acquity UPLC HSS T3 (100×2.1 mm, Waters) and the mobile phases were (A) H_2O + formic acid 0.05% and (B) acetonitrile + formic acid 0.05%. The flow rate was 0.5 mL min^{-1}. The column temperature was set at 25°C. The gradient program was as follows: 0-100 % B in 10 min, hold at 100% for 2 min, and re-equilibration at 2% B for 3.0 min. The injection volume was 1 μL. The high-resolution mass spectrometer was operated in both positive and negative electrospray ionization using the MS^E mode over a mass range of 50-1200 Da. MS^E collected data without preselection of parent ions by alternatively switching from low (4 eV) to high (ramp of 10-60 eV) collision energies. The following source conditions were used: capillary voltage +1 kV/-1 kV, cone voltage +25 V/-25V, source temperature 140°C, desolvation temperature 500°C, desolvation gas flow 1000 L h^{-1}, and cone gas flow 150 L h^{-1}. Data were acquired in centroid mode with a resolution of ca. 23,000 (at *m/z* 556.2766). The scan time was set to 0.2 s for both low and high collision energy functions. Internal calibration was performed through the Lockspray probe by infusing a 50 ng mL^{-1} solution of leucine-enkephalin in the mass spectrometer at a flow-rate of 10 μL min^{-1}. The system was controlled by Masslynx 4.2 (Waters, Milford, MA, USA). The quantification of glucosinolates and their breakdown products was carried out in a relative manner. The predominant glucosinolates in *Arabidopsis* veins (glucoraphanin, glucoiberin, glucoalyssin) and their corresponding isothiocyanate breakdown products were analysed with TargetLynx software (Waters, Milford, MA, USA), and the integrated peak areas were normalized to the initial plant mass.[52] At least 4 independent replicates were used for each treatment. Chemical structures were drawn with ChemDraw v20.0 software (PerkinElmer, Waltham, Massachusetts, USA).

Western blotting

Recombinant TGG1-StrepII-9×His (10 μM) in 50 mM MES, pH 6.0 with Tris, was applied to wild-type plants by cutting the scalded petiole 8 while it was immersed in this solution. Distal leaf 13 (including the petiole) was collected 5 min after protein application, then ground into powder in liquid nitrogen and centrifuged at 12,000 g at 10°C for 10 min. The supernatant was collected and stored at -80°C for further use. 10 μL of this extract was mixed with 6× loading buffer (12% sodium dodecyl sulfate, 60% glycerol, 0.6 M dithiothreitol, 0.06% bromophenol blue in 0.375 M Tris-HCl, pH 6.8) and boiled for 5 min prior to loading into a SDS-PAGE gel (10% acrylamide). Proteins were then transferred to nitrocellulose blotting membranes (Amersham Protran 0.45 μm, Cytiva, Glattbrugg, Switzerland) with Pierce™ 1-step transfer buffer and Pierce™ power blotter (Thermo Fisher Scientific, Reinach, Switzerland). The nitrocellulose membrane was then incubated overnight at 4°C with Western Blocking Reagent (Roche, Basel, Switzerland) diluted

1:10 (v/v) with Tris-buffered saline/Tween 20 (TBST; 20 mM Tris-HCl, pH 7.5, 150 mM NaCl, and 0.05% (v/v) Tween 20). The membrane was washed consecutively with 3×10 mL TBST, 10 min each wash. After washing, the nitrocellulose membrane was incubated for 2 h at room temperature (24°C) with Anti-His_6-Peroxidase (Roche, Basel, Switzerland) diluted 1:2000 (v/v) with TBST. Excess antibodies were removed with 3×10 mL TBST washes, 10 min each. The WesternBright Sirius HRP substrate (Advansta, Menlo Park, CA, USA) was then added to the membrane. Chemiluminescence/images were collected with an ImageQuant LAS 500 (Cytiva, Glattbrugg, Switzerland). Western blots were performed three time independently with similar results.

QUANTIFICATION AND STATISTICAL ANALYSIS

Electrical signal quantification was performed using LabScribe4 software (iWorx Systems, Inc.). Fluorescent images were analyzed with Fiji/ImageJ, contrast and brightness adjustment were applied in the same manner for all images in the same experiment. No data were excluded. GraphPad Prism 8.0.2 (263) and SigmaPlot 14.0 were used for graph plotting. Statistical analyses and data fitting were performed with GraphPad Prism 8.0.2 (263). Unpaired two-tailed Student's *t*-test was performed when comparing only two groups. One-way ANOVA followed by Tukey's test was used as a multiple comparison procedure when comparing one variable across multiple groups. In graphs with error bars, data are shown as mean ± standard deviation (SD) and *p* values are indicated.

CellPress
OPEN ACCESS

Supplemental figures

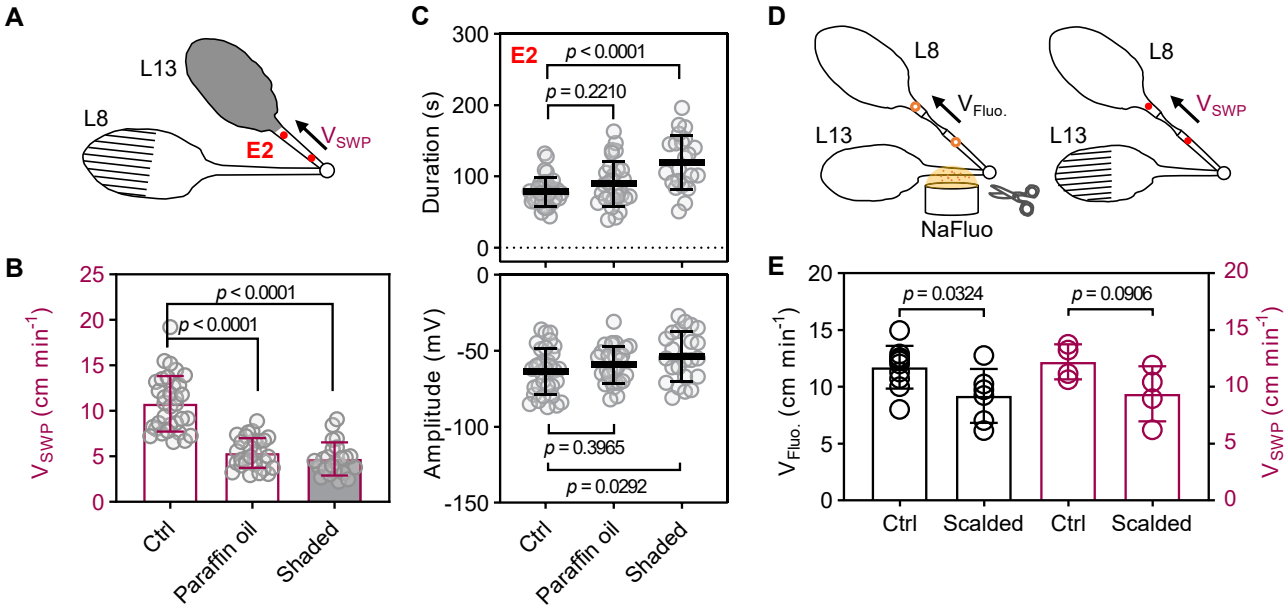

Figure S1. Slow wave potential velocity and chemical propagation in shaded or scalded *Arabidopsis*, related to Figures 1 and 2

(A) Experimental design for wound-induced SWP propagation analysis. Red dots, electrodes; leaf 8 was wounded 3 h after covering both side of leaf 13 with paraffin oil or shading with aluminum foil.

(B and C) (B) Velocity and (C) duration and amplitude of SWP in the petiole of leaf 13 (n = 23–33, means ± SD, one-way ANOVA followed by Tukey's test). SWPs shown in (C) were recorded at E2. The control (Ctrl) plants were not shaded or paraffin-treated.

(D) Experimental design for NaFluo and SWP propagation analyses. WT plants were used 3 h after scalding. The control plants did not have leaf 8 scalds. Fluorescence from two regions of interest in petiole 8 (open circles) were used for velocity calculation; SWPs recorded with two electrodes (red dots) were analyzed for velocity calculation.

(E) Velocity of NaFluo and SWP propagation through scalded petioles (means ± SD; n = 4–10; unpaired two-tailed Student's t test).

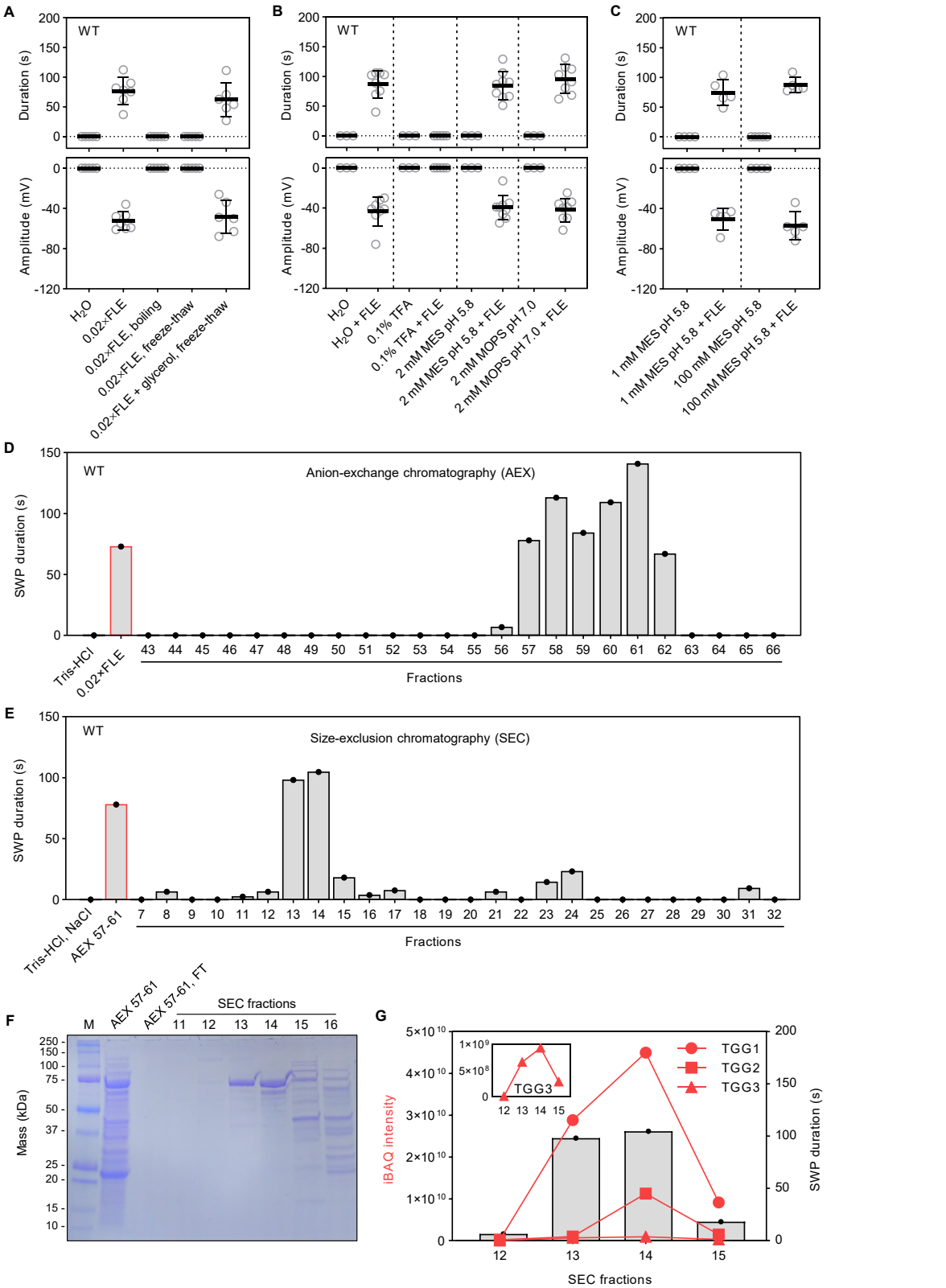

(legend on next page)

Figure S2. Properties, fractionation, and identification of Ricca's factors in *Arabidopsis*, related to Figure 3

(A) SWPs induced by 0.02 × fresh leaf extract (FLE) in WT plants after 5 min boiling or 3 consecutive freeze-(10 min) thaw (10 min) cycles with or without 50% (v/v) glycerol. In each case undiluted FLE was subjected to a treatment then diluted 50-fold with H_2O prior to bioassay (means ± SD; n = 5–7).

(B) SWPs induced by 0.02 × FLE in WT plants after dilution of 1 × FLE with different pH buffers (means ± SD; n = 3–9). pH adjusted with NaOH.

(C) SWPs induced by 0.02 × FLE in WT plants after dilution of 1 × FLE with 1 mM or 100 mM MES buffer, pH 5.8 with NaOH (means ± SD; n = 4–5).

(D) Activity of fractions from DEAE anion-exchange chromatography (AEX) in the Ricca assay. Tris-HCl (50 mM Tris-HCl, pH 8.0), negative control; 0.02 × FLE, fresh leaf extract sample was diluted 50-fold with Tris-HCl as positive control (activity is shown as means of SWP duration; n = 1–3).

(E) Activity of fractions from size-exclusion chromatography (SEC) in the Ricca assay. Active fractions 57–61 in (D) were combined, buffer exchanged, and fractionated by SEC in 50 mM Tris-HCl, pH 8.0, 200 mM NaCl. AEX 57–61, buffer exchanged AEX 57–61 as positive control (activity is shown as means of SWP duration; n = 1–4).

(F) SDS-PAGE of AEX 57–61 (buffer exchanged AEX 57–61), "AEX 57–61, FT" (flow through of AEX 57–61 during buffer exchange process), and SEC fractions 11–16 from (E).

(G) Intensity-based absolute quantification (iBAQ) of peptides from TGG1, TGG2, and TGG3, and activity of SEC fractions 12–15, as shown in (E). FLE from WT plants was used. Solution was supplied through scalded petiole 8 of WT plant and electrical signals in distal leaf 13 petiole were monitored.

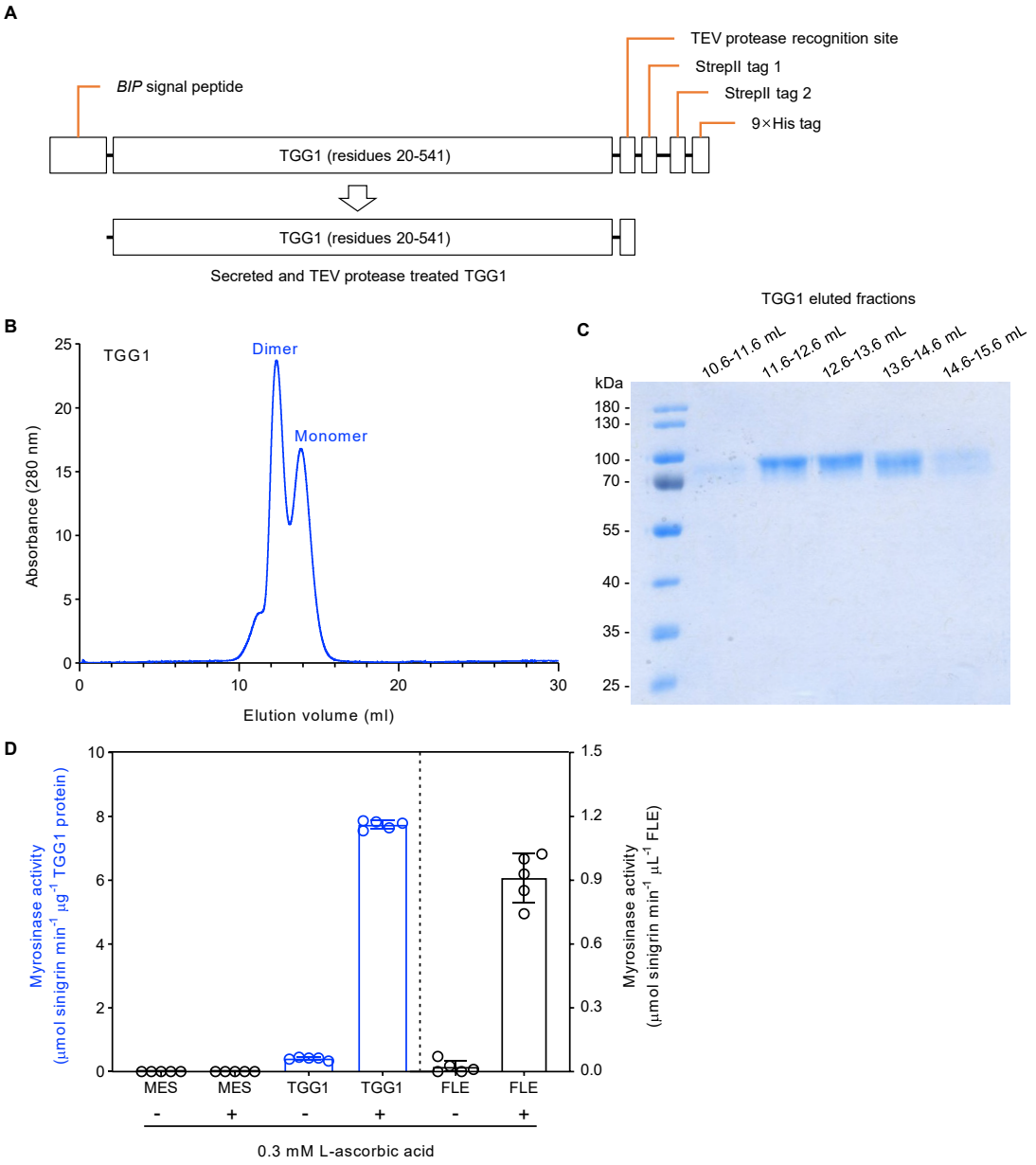

Figure S3. Purification and enzyme activity of recombinant TGG1, related to Figure 4

(A) Strategy for producing recombinant TGG1 from insect cells.

(B) Size-exclusion chromatography (SEC) profile of recombinant TGG1 protein. The chromatogram recorded at 280 nm shows two main peaks, corresponding to apparent molecular masses of approximately 200 and 100 kDa for peak 1 (dimer) and peak 2 (monomer), respectively. The column was calibrated with protein standards.

(C) SDS-PAGE of TGG1 fractions eluted from SEC. The volume of each fraction was 1 mL.

(D) Myrosinase activity of TGG1 and WT plant FLE (means ± SD, n = 5). Assays were performed at pH 6.0 in 50 mM MES buffered with Tris.

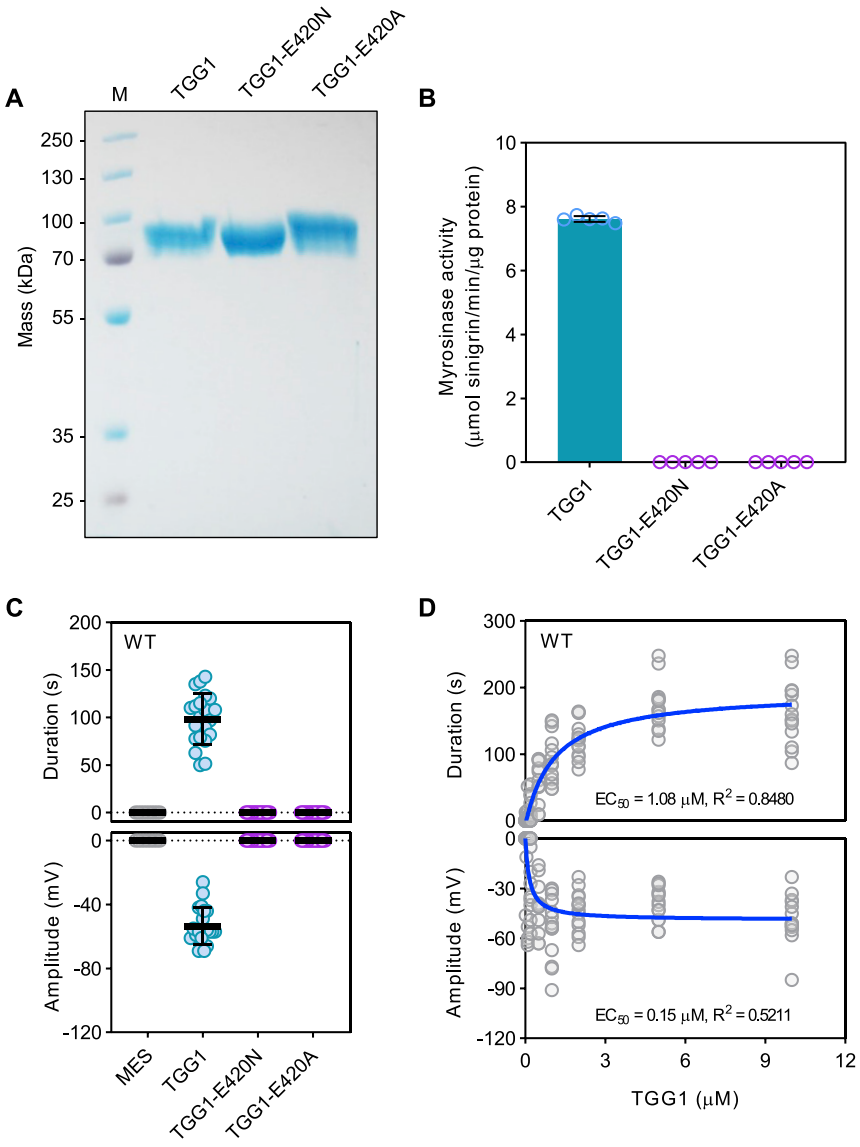

Figure S4. Catalytically inactive TGG1 variants, related to Figure 4

(A) SDS-PAGE of purified TGG1 variants. 5 μg of each protein was loaded prior to electrophoresis under denaturing conditions.

(B) Myrosinase activity of TGG1 variants (means ± SD; n = 5).

(C) Mutated TGG1 (1 μM) failed to induce SWPs in WT plants (means ± SD; n = 10–21). Each recombinant protein was supplied through scalded petiole 8 of WT plant and electrical signals in distal leaf 13 petiole were monitored.

(D) EC_{50} for TGG1-induced SWP durations and amplitudes in WT plants. Fitting of the data from Figure 4C (n = 4–14). EC_{50}, concentration for 50% of maximal effect.

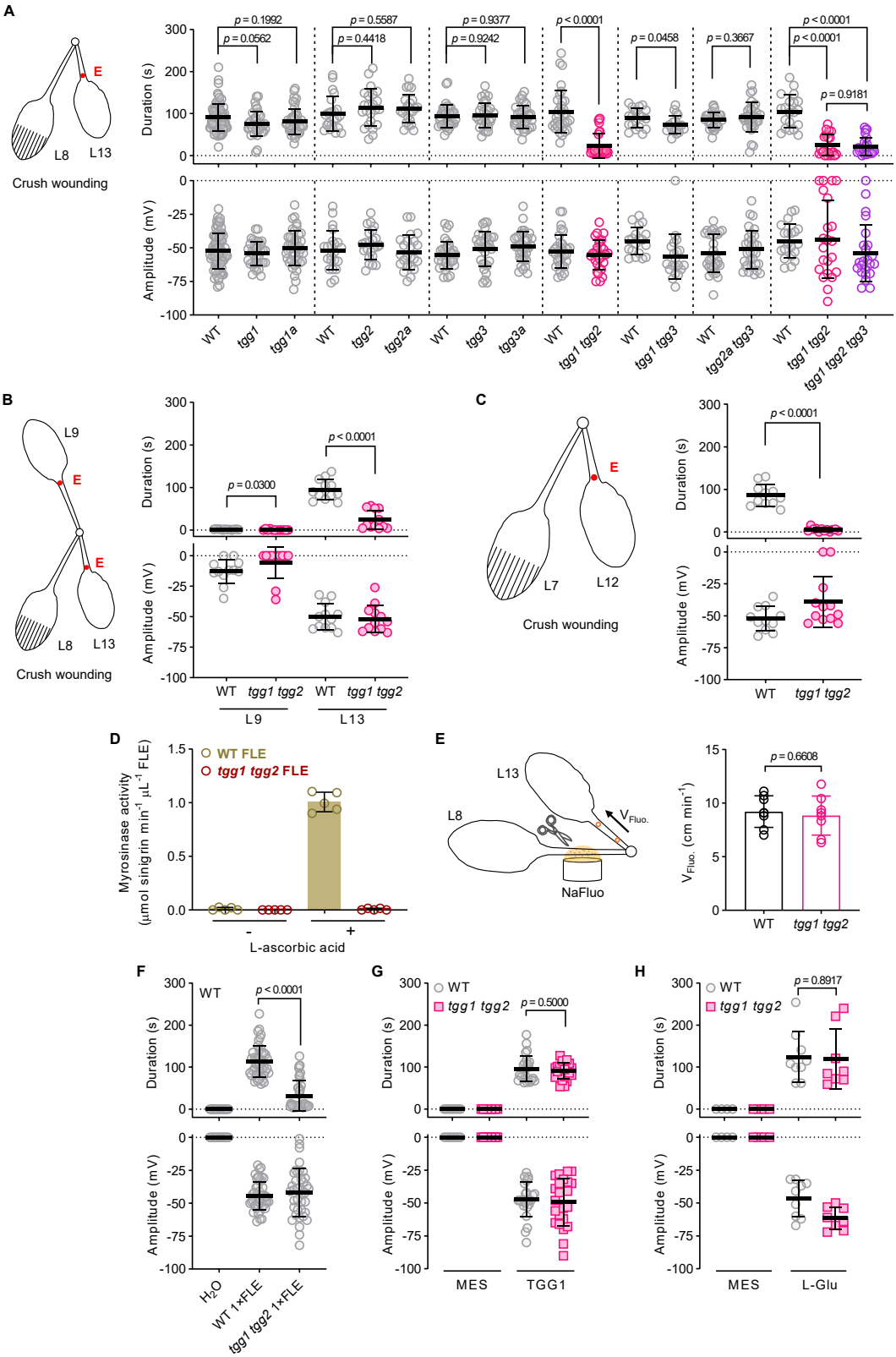

(legend on next page)

Figure S5. TGGs mediate leaf-to-leaf slow wave potentials, related to Figure 4

(A) Experimental design for crush wound-induced electrical signal detection (left; red dot, surface electrode) and wound-induced slow wave potentials (SWPs) in *tgg* mutants (right; n = 18–79).

(B) Experimental design for crush wounding leaf 8 and electrical signal detection in leaf 9 and leaf 13 (left; red dot, surface electrode) and crush wounding-induced SWPs (right, n = 12).

(C) Experimental design for crush wounding leaf 7 and electrical signal detection in leaf 12 (left; red dot, surface electrode) and crush wounding-induced slow wave potentials (right, n = 11–12).

(D) Myrosinase activity of fresh leaf extract from WT and *tgg1 tgg2* with and without 0.3 mM L-ascorbic acid (n = 5).

(E) Experimental design for NaFluo loading (left), and velocity of NaFluo propagation in WT and *tgg1 tgg2* (right; n = 8).

(F) Fresh leaf extract from *tgg1 tgg2* failed to induce WT-like SWPs when applied to WT plants (n = 17–47).

(G) TGG1-induced SWPs in *tgg1 tgg2* (n = 9–24). TGG1 was diluted with 50 mM MES, pH 6.0 with Tris to 1 μM prior to application.

(H) L-Glu-induced SWPs in *tgg1 tgg2* (n = 4–9). 5 mM L-glutamic acid in 50 mM MES, pH 6.0 with Tris was applied.

For (F)–(H), solutions of FLE, TGG1 or L-glutamic acid (L-Glu) were supplied through scalded petiole 8 and electrical signals in distal leaf 13 petiole were monitored. Data are means ± SD; unpaired two-tailed Student's t test or one-way ANOVA followed by Tukey's test for multiple comparisons.

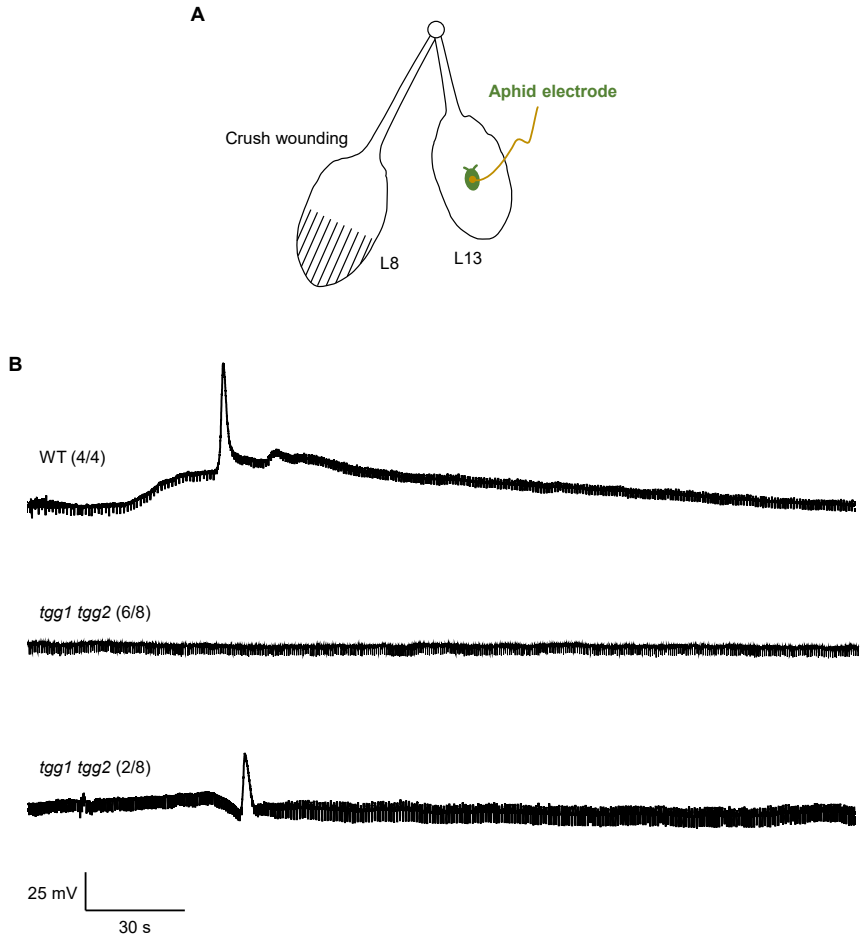

Figure S6. Wound-response phloem electrical signals depend on TGG1/2, related to Figure 5

(A) Experimental design for electrical penetration graph (EPG) recordings from sieve elements. Green indicates the aphid electrode.

(B) Representative EPG recordings from WT and *tgg1 tgg2* sieve elements. Data in parentheses represent the number of typical recordings/total recordings.

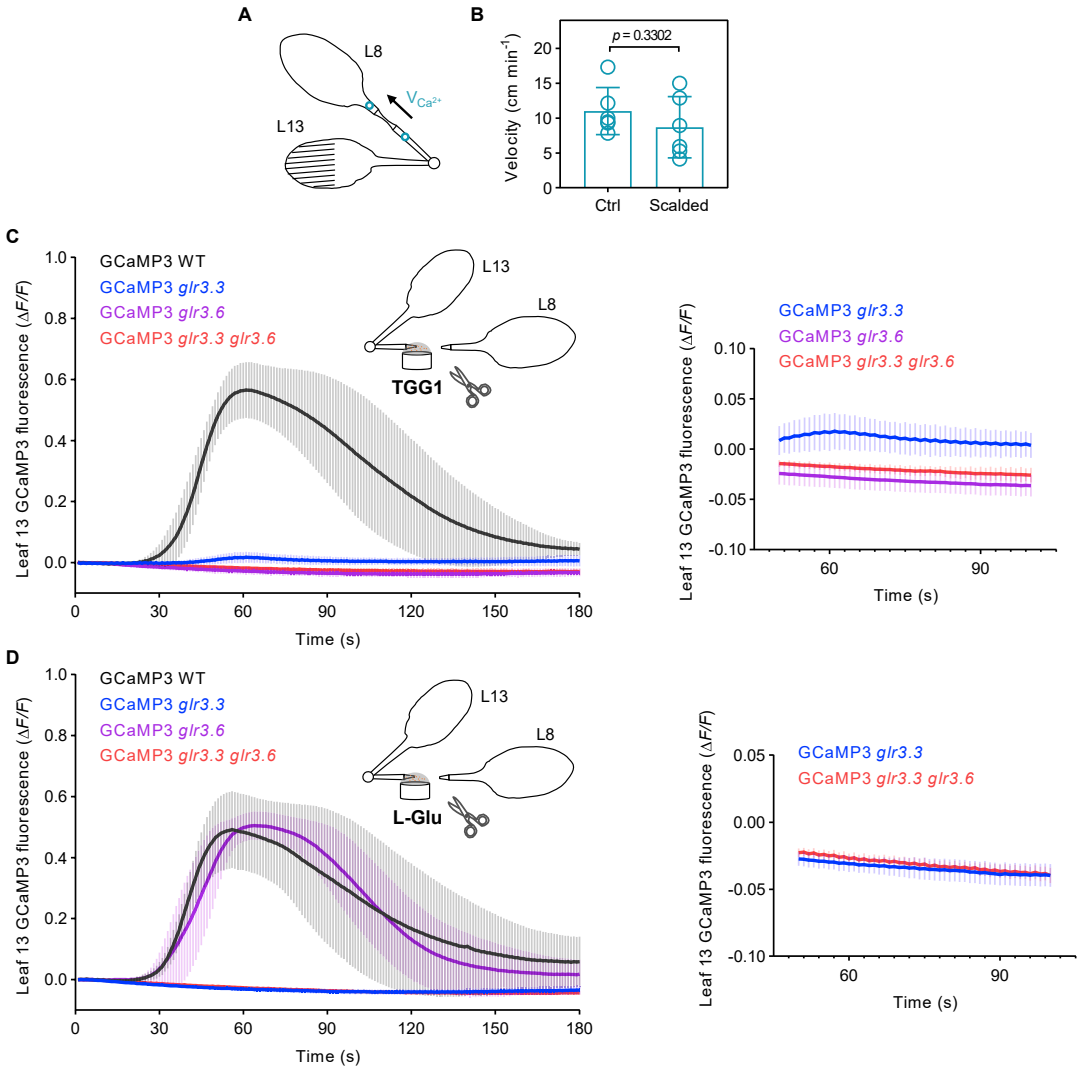

Figure S7. Cytosolic Ca^{2+} transients induced by wounding, TGG1, and L-glutamate, related to Figure 5

(A) Experimental design for Ca^{2+} signal velocity analyses. GCaMP3 WT plants were used 3 h after scalding. The control plants did not have leaf 8 scalds. Fluorescence from two regions of interest in petiole 8 (open circles) was used for velocity calculation.

(B) Apparent velocity of Ca^{2+} signal propagation through control and scalded petioles (means ± SD; n = 6; unpaired two-tailed Student's t test).

(C) Recombinant TGG1-induced cytosolic Ca^{2+} transients in GCaMP3-expressing plants (left) and magnified plot (right; means ± SD; n = 9). Inset, experimental design for TGG1 loading. Recombinant TGG1 protein (1 μM) in 50 mM MES, pH 6.0 with Tris was fed through the scalded petiole of leaf 8 and GCaMP3 fluorescence from leaf 13 (petiole and lamina) was analyzed.

(D) L-Glu-induced cytosolic Ca^{2+} transients in GCaMP3-expressing plants (left) and magnified plot (right; means ± SD; n = 8–9). Inset, experimental design for L-Glu loading. 5 mM L-glutamic acid in 50 mM MES, pH 6.0 with Tris was fed through the scalded petiole of leaf 8 and GCaMP3 fluorescence from leaf 13 (petiole and lamina) was analyzed.

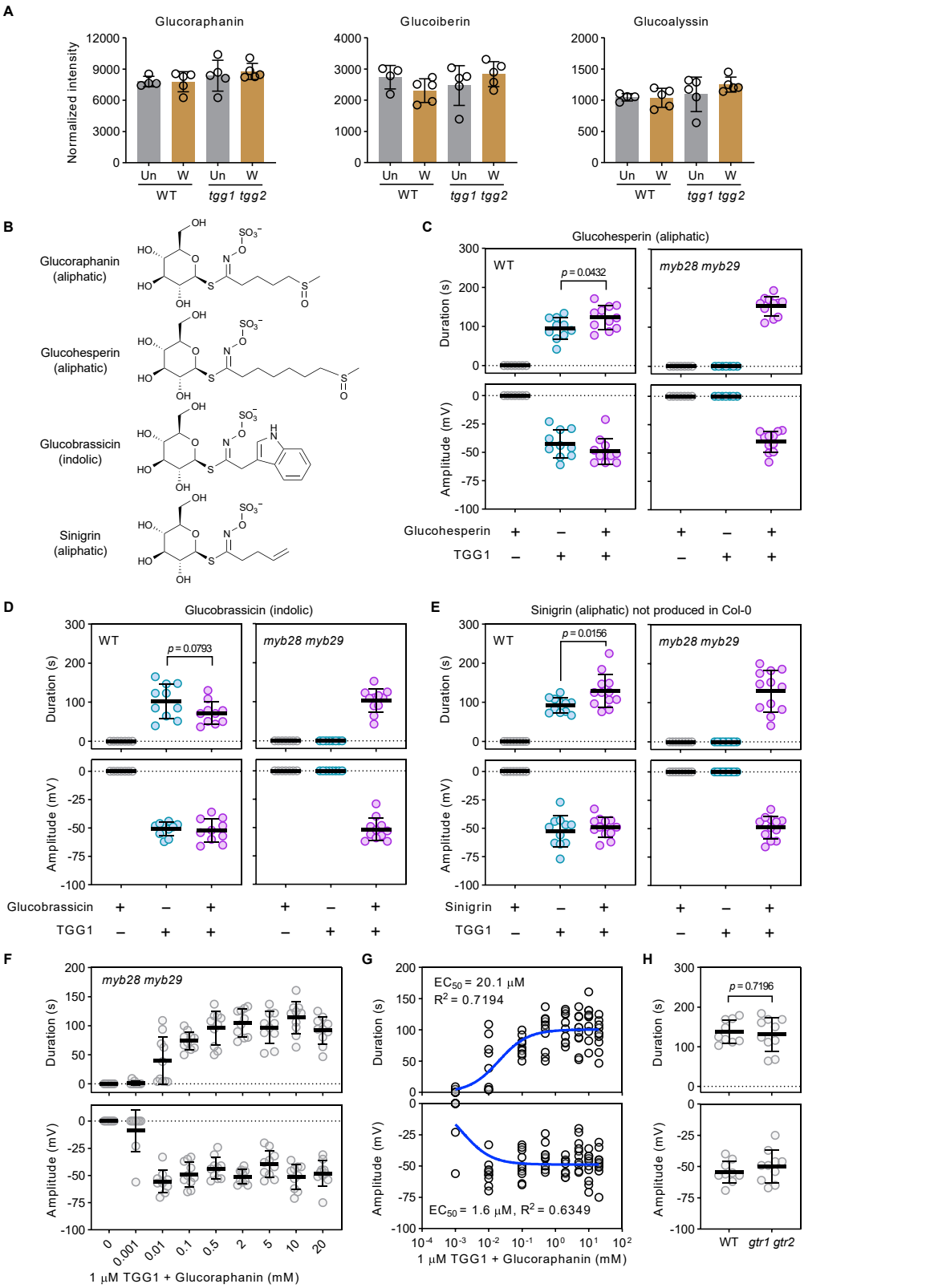

(legend on next page)

Figure S8. Breakdown products from aliphatic and indolic glucosinolates induce SWPs in distal leaf 13, related to Figure 6

(A) Analyses of aliphatic glucosinolates in the midveins of unwounded (Un) and wounded (W) plants (n = 4–5). For wounded plants, midveins from leaf 13 were sampled 2 min after crush wounding leaf 8.

(B) Structural formulae of glucosinolates.

(C) TGG1 and glucohesperin breakdown products induce slow wave potentials (SWPs) in distal leaf 13 (n = 7–11).

(D) TGG1 and glucobrassicin breakdown products induce SWPs in distal leaf 13 (n = 7–11).

(E) TGG1 and sinigrin breakdown products induce SWPs in distal leaf 13 (n = 8–12). Data are means ± SD; unpaired two-tailed Student's t test.

(F) Dose-response for glucoraphanin activity at different concentrations at the presence of 1 μM TGG1 (means ± SD; n = 8–10).

(G) EC_{50} (50% of maximal effect) for glucoraphanin breakdown product-induced SWP durations and amplitudes (n = 8–10). Fitting of the data from (F).

(H) Wound-induced SWPs in *gtr1 gtr2* mutants (means ± SD; n = 9–10; unpaired two-tailed Student's t test).

For (C)–(E), glucosinolates were fed through the scalded petiole of leaf 8 at a concentration of 10 mM; TGG1 was fed at a concentration of 1 μM; electrical signals were monitored on distal leaf 13 of WT or *myb28 myb29* plants.